

THIS REPORT HAS BEEN DELIMITED  
AND CLEARED FOR PUBLIC RELEASE  
UNDER DOD DIRECTIVE 5200.20 AND  
NO RESTRICTIONS ARE IMPOSED UPON  
IT'S USE AND DISCLOSURE.

DISTRIBUTION STATEMENT A

APPROVED FOR PUBLIC RELEASE,  
DISTRIBUTION UNLIMITED.

# Armed Services Technical Information Agency

Because of our limited supply, you are requested to return this copy WHEN IT HAS SERVED YOUR PURPOSE so that it may be made available to other requesters. Your cooperation will be appreciated.

AD

45686

NOTICE: WHEN GOVERNMENT OR OTHER DRAWINGS, SPECIFICATIONS OR OTHER DATA ARE USED FOR ANY PURPOSE OTHER THAN IN CONNECTION WITH A DEFINITELY RELATED GOVERNMENT PROCUREMENT OPERATION, THE U. S. GOVERNMENT THEREBY INCURS NO RESPONSIBILITY, NOR ANY OBLIGATION WHATSOEVER; AND THE FACT THAT THE GOVERNMENT MAY HAVE FORMULATED, FURNISHED, OR IN ANY WAY SUPPLIED THE SAID DRAWINGS, SPECIFICATIONS, OR OTHER DATA IS NOT TO BE REGARDED BY IMPLICATION OR OTHERWISE AS IN ANY MANNER LICENSING THE HOLDER OR ANY OTHER PERSON OR CORPORATION, OR CONVEYING ANY RIGHTS OR PERMISSION TO MANUFACTURE, USE OR SELL ANY PATENTED INVENTION THAT MAY IN ANY WAY BE RELATED THERETO.

Reproduced by  
DOCUMENT SERVICE CENTER  
KNOTT BUILDING, DAYTON, 2, OHIO

UNCLASSIFIED

AD NO. ~~43686~~

ASTIA FILE COPY

TECHNICAL REPORT NO. 6418-7

AN INEXPENSIVE SUPERSONIC  
WIND TUNNEL FOR HEAT-TRANSFER  
MEASUREMENTS

PART I — APPARATUS, DATA, AND RESULTS FOR A LAMINAR BOUNDARY LAYER  
BASED ON A SIMPLE ONE-DIMENSIONAL FLOW MODEL

BY

JOSEPH KAYE, JOSEPH H. KEENAN, GEORGE A. BROWN,  
AND ROBERT H. SHOULBERG

FOR

OFFICE OF NAVAL RESEARCH

CONTRACT N5ori-07805

NR-061-028

D. I. C. PROJECT NUMBER 6418

JUNE 1, 1954

---

MASSACHUSETTS INSTITUTE OF TECHNOLOGY

DEPARTMENT OF MECHANICAL ENGINEERING

AND

DIVISION OF INDUSTRIAL COOPERATION

CAMBRIDGE, MASSACHUSETTS

BEST AVAILABLE COPY

# AN INEXPENSIVE SUPERSONIC WIND TUNNEL FOR HEAT-TRANSFER MEASUREMENTS

Part I - Apparatus, Data, and Results for a Laminar Boundary Layer  
Based on a Simple One-Dimensional Flow Model

By

Joseph Kaye,<sup>1</sup> Joseph H. Keenan,<sup>2</sup> George A. Brown,<sup>3</sup> and Robert H. Shoulberg.<sup>4</sup>

## SUMMARY

Reliable experimental data, obtained at relatively low cost, are presented in the form of heat-transfer coefficients for air moving at supersonic speeds in a round tube. These data are analyzed, interpreted, and compared with available data in the literature.

The experimental local heat-transfer coefficients are for laminar, transitional, and turbulent boundary layers. The data for a laminar boundary layer are given in this paper, and the remaining data will be given in a separate paper. The experimental data for 17 runs are given here for Mach numbers at tube inlet of 2.8 and 3.0. The range of values of diameter Reynolds number covered is from 20,000 to 100,000 for these laminar flow tests, while the length Reynolds number extends to about 4,000,000. The computed quantities are obtained on the basis of a simple one-dimensional flow model, but a subsequent paper will analyze the same data in greater detail on the basis of a two-dimensional flow model.

<sup>1</sup>Associate Professor of Mechanical Engineering, Massachusetts Institute of Technology.

<sup>2</sup>Professor of Mechanical Engineering, Massachusetts Institute of Technology.

<sup>3</sup>Shell Fellow in Mechanical Engineering, Massachusetts Institute of Technology.

<sup>4</sup>M. W. Kellogg Company, New York, New York.

## NOMENCLATURE

$A$	- cross-sectional area, $\pi D^2/4$
$A'$	- heat-transfer area, $\pi D \Delta L$
$c_p$	- specific heat at constant pressure
$c_v$	- specific heat at constant volume
$c_w$	- discharge coefficient of nozzle
$D$	- inside diameter of pipe
$g$	- acceleration given to unit mass by unit force
$G$	- flow per unit area, $w/A$
$h$	- coefficient of heat transfer, $q/A'(t_w - t_{aw})$
$k$	- ratio of specific heats, $c_p/c_v$
$L$	- distance from end of curved contour of nozzle
$M$	- Mach number, $V/\sqrt{gkRT}$
$n$	- summation index, Eq. (8)
$Nu_D$	- diameter Nusselt number, $hD/\lambda_m$
$Nu_L$	- length Nusselt number, $hL/\lambda_m$
$p$	- static pressure
$q$	- rate of heat transfer
$r$	- recovery factor, $(t_{aw} - t_m)/(t_{oi} - t_m)$
$R$	- perfect-gas constant
$Re_D$	- diameter Reynolds number, $DG/\mu g$
$Re_L$	- length Reynolds number, $LG/\mu g$
$St$	- Stanton number, $h/c_p G$
$t$	- temperature, deg F
$T$	- temperature, deg F abs
$V$	- velocity
$w$	- mass rate of flow
$\rho$	- density
$\mu$	- viscosity
$\lambda$	- thermal conductivity

Superscript \* refers to throat of supersonic nozzle where  $M = 1$

### Subscripts:

aw	- adiabatic wall conditions
j	- station numbers
m	- mean stream conditions
o	- hypothetical entrance plane of the tube, where the boundary layer is of zero thickness
of	- downstream stagnation conditions
oi	- upstream stagnation conditions
oj	- local stagnation conditions at station j
r	- atmospheric conditions
s	- isentropic conditions
w	- wall conditions
$\infty$	- free stream conditions for flat-plate flow

## INTRODUCTION

A wind tunnel is usually considered to be a device in which models may be inserted and tested under controlled conditions. Wind tunnels have been also used, however, to study basic phenomena in fluid mechanics, such as boundary-layer mechanics, turbulence, stability of the laminar boundary layer, interaction of shock waves and boundary layers, and, in more recent years, heat-transfer phenomena in supersonic flow. Most supersonic wind tunnels which are large enough to insert models of reasonable size are expensive to build and to operate, and also expensive when used to measure heat-transfer data for supersonic flow. Supersonic flow established under controlled conditions in a small round tube, one-half inch in diameter can be used to measure local heat-transfer coefficients. The corresponding apparatus, which is described herein, may be considered to be an example of an inexpensive supersonic wind tunnel, in that it is both relatively cheap to design and construct, and also, relatively low in operational costs.

A recent survey (1)\* has shown the great need for reliable heat-transfer data for supersonic flow in view of the small amount of such data published during the years from 1948 to 1953. For this reason a fairly detailed account of the results obtained in an investigation of heat-transfer coefficients for supersonic flow of air in a round tube is to be presented in a series of papers. The first paper, which is the present one, consists of a description of the two sets of apparatus used, the original data, and the calculated results for a laminar boundary layer based on a simple one-dimensional flow model. The second paper will present the calculated results for a laminar boundary layer based on a two-dimensional flow model for the entrance region of a tube. The third paper will present the original data and the calculated results for a transitional and for a turbulent boundary layer based on a simple one-dimensional flow model.

The present investigation of heat-transfer coefficients for supersonic flow of air in a round tube was started some seven years ago under the sponsorship of the Office of Naval Research. Preliminary data and results were obtained several years ago with the first apparatus, described herein as test combination C. Similar results were not then available in the literature for comparison. The possibility of systematic errors in the data and the lack of knowledge of the type of boundary layer which existed in the supersonic flow of air in the tube were two main reasons for designing, building, and testing a new apparatus to get more reliable heat-transfer coefficients for supersonic flow.

\*Numbers in parentheses refer to the Bibliography at the end of the paper.

In the last few years the results obtained for supersonic flow of air in a round tube, with and without heat transfer to the air stream, have been placed on a firm foundation as indicated by the following evidence:

1. The experimental data obtained by different teams of students working with different test combinations, for both adiabatic and diabatic flow, have shown the absence of significant systematic errors.
2. The nature of the boundary layer present in the tube flow has been conclusively demonstrated by means of accurately measured velocity profiles (2,3).
3. The accurately measured velocity profiles for supersonic flow in the tube have also demonstrated the basic soundness of the two-dimensional flow model used to interpret the data.
4. Theoretical solutions (4) have been obtained for the system of partial differential equations of energy, momentum, and continuity for the case of supersonic flow of air in a tube in the entrance region. These solutions describe the behaviour of supersonic flow in a tube with a laminar boundary layer developing from the entrance plane of the tube.

#### METHODS OF TESTING

The experimental program described here has consisted of two parts. In the first part, a well-insulated round tube was used to measure values of the local adiabatic wall temperature and local static pressure of a supersonic stream of air. The results of these tests, with a complete description of the apparatus, are given in references (5) and (6). In order to minimize the amount of repetition, the reader is referred to these two papers for many details not given in this paper. In the second part of the program, two different test combinations were used in which steam was condensed outside a round brass tube in order to measure the local coefficient of heat transfer to a supersonic stream of air flowing inside the tube.

The general preparation of the air flow and the method of drying the air stream are given in detail in reference (5). These are the same for both parts of the program. The schematic layout of the entire flow system is shown in Fig. 1. The purpose of the major changes made for the tests with diabatic flow was to insure that almost saturated or slightly superheated steam entered the outer steam chest of the apparatus and to minimize the heat losses from the apparatus to the surroundings.

A major difference between tests for adiabatic and diabatic flow was the length of time required to bring the large mass of heat-transfer apparatus up to a fixed temperature corresponding to that of the condensing steam. This transient heating process was carefully observed and recorded in the diabatic tests until a steady-state condition was obtained. Heat-transfer measurements were made only for the steady state. During the large time interval required for both the transient process and the measurements, the conditions in the steam main varied only slowly. Control devices were found necessary to superheat or desuperheat the steam only slightly in order to maintain constant the state of the steam fed to the steam chest of the apparatus. They are indicated in the schematic layout of Fig. 1. The measured superheat was found to be about  $0.5^{\circ}\text{F}$  on the average.

### EXPERIMENTAL APPARATUS

Some salient features of the two test combinations of heat-transfer apparatus are described in Table 1. The length-diameter ratio in Table 1 is based on the distance from the end of the curved contour of the supersonic nozzle to the exit plane of the test section.

TABLE 1

TEST COMBINATIONS OF HEAT-TRANSFER APPARATUS

SYMBOL	NOZZLE	TEST SECTION	L/D	$M_o$
C	Brass	Brass	31.8	3.0
D	Stainless steel	Brass	49.8	2.8

The nozzles used to produce supersonic flow in test combinations C and D were different in design and in final contour. Details of design and of construction of these two nozzles are shown in reference (5). For purposes of illustration, the rough dimensions and shapes of these two nozzles are shown in Fig. 2. In the brass nozzle of test combination C, no means of measuring the temperature gradient along the axial length was available, whereas two thermocouples were installed in the stainless-steel nozzle to determine the axial temperature gradients for test combination D.

#### Design Considerations for Test Sections

The first test section, used in test combination C was designed to produce a small thermal resistance for radial heat flow through the tube wall in comparison with the thermal resistance being measured, namely, that from the wall to the air stream in the tube. Brass was therefore



selected for the tube material. The temperature of the tube was maintained constant over its entire length by surrounding it with condensing steam.

The experience gained after operation of test combination C for about two years resulted in the following additional design requirements for test combination D:

1. The joint between the nozzle and collar, and that between the collar and test section should be made as nearly perfect as possible. A misfit in excess of 0.0002 in. in the diameter of 0.5 in. is undesirable.
2. The axial heat flow from the hot test section to the cooler nozzle should be reduced to a minimum. This objective was achieved in test section D by use of a nozzle and a collar made of stainless steel which has a considerably lower thermal conductivity than that of brass.
3. The no-load or blank-run condensation rate, which is determined by flow of steam into the steam chest for zero flow of air in the test section and which is an indication of the total amount of undesired heat flow from the steam to the surroundings, should be minimized, especially when a laminar boundary layer is established in the test section.
4. The state of the steam entering the steam chest must be carefully controlled to be slightly superheated, and the steam flow distribution into and within the steam chest must be as nearly uniform as practical.

#### Test Apparatus

In order to minimize repetition, the general common features of test combinations C and D will be described first. The dried air stream leaves the upstream stagnation tank, passes through the supersonic nozzle into the half-inch test section of brass, and then passes out through the downstream stagnation tank into the ejector to the atmosphere. Steam drawn from the supply main passes through a trap, a pressure regulator, a combination of a desuperheater and a superheater with electrical heat input, enters the steam chest through the inlet pipe, and is distributed around the test section. The steam is prevented from flowing directly to the outside of the test section by means of a brass semicylindrical umbrella which covers the entire length of the tube. This umbrella serves to prevent any condensate other than that formed on the tube from entering the compartments around the test section. It serves also as a radiation shield.

The outside of the test section is partly surrounded by a semicylindrical brass trough, open at the top. This trough is subdivided into

compartments by means of thin brass partitions set perpendicular to the tube axis at definite intervals. The steam in contact with the tube wall in a given compartment condenses at a rate proportional to the rate of heat transfer to the air flowing inside the tube. This condensate is caught in the trough and drains from the compartment through a short piece of neoprene tubing into a steam-jacketed, calibrated, and graduated glass collecting tube. The glass collecting tubes are shielded from the atmosphere by highly reflective aluminum foil.

The entire test section, together with nozzle and stagnation tanks, is covered with a large thickness of insulating felt and then with aluminum foil to reduce extraneous heat flows. The total thermal capacity of this insulation, the test section, and the surrounding steam chest is quite large, so that a large amount of steam condenses in the transient warm-up process before the steady-state measurements of heat transfer are made. Drains for removing the condensate and atmospheric vents to speed up preliminary heating were provided in both test combinations.

The method of construction of the test section was almost the same for the two test combinations. An axial hole was drilled in a solid brass rod and then the numerous holes for pressure taps were drilled through the wall of the tube. The inside surface of the tube was prepared by successive polishing operations alternating with successive cleanings of the pressure-tap holes, until a high polish was present on the inside surface with no detectable burrs at the pressure taps. The angular position of the pressure-tap holes was rotated from the entrance of the tube to the exit.

The steam chest for test combination C was almost square in cross section and was made from welded plates, except for two sides. The chest for test combination D was made from a circular casting, with two halves joined by bolts at a gasket, in order to be able to increase the working pressure of the steam in the chest.

The measurements made for both test combinations C and D included the upstream stagnation temperature and pressure, the tube-wall temperature along its entire length, the local static pressure of the air flow, the local rate of collection of condensate from each compartment, the downstream stagnation temperature and pressure, the no-load condensate rate for zero air flow, and the pressure and temperature of the steam at several locations in the steam jacket.

#### Test Combination C

The details of test combination C are shown in Fig. 3. Photographs of this apparatus, before and after assembly, are shown in Figs. 4 and 5.

respectively. The compartments of the condensate-collecting trough are clearly visible in Fig. 4. The protecting umbrella is clearly visible in Fig. 5, which also shows the pressure connections, the condensate tubing, and steam-jacketed glass collecting tubes. The upstream stagnation tank is to the left in Fig. 5. The important dimensions of test combination C are summarized in Appendix A.

When test combination C was first assembled, a hard rubber collar was used between the nozzle and the test section. The first twelve runs (K-1 through K-12) yielded pressure distributions which were not as smooth as those obtained for the measurements with adiabatic flow. The nozzle and collar were taken apart and it was found that they were misaligned by about 0.001 in. A new collar was prepared and the joint between nozzle and collar and that between collar and test section were carefully polished and aligned. The remaining heat-transfer runs made with test combination C were found to yield smooth pressure distributions, indicating the achievement of smooth flow at the entrance of the test section.

#### Test Combination D

The details of test combination D are shown in Fig. 6. Photographs of this apparatus, before and after assembly, are shown in Figs. 7 and 8, respectively. Fig. 7 shows clearly the stainless-steel supersonic nozzle, the collar, the test section with the surrounding compartments, the large castings for the steam chest, and, finally, the downstream stagnation tank. Fig. 8 shows the connections for the pressure leads, for the thermocouples in the test section, and for the condensate collecting tubes.

Test combination D differed from C mainly in the use of a longer test section. The length-diameter ratio for D is 49.8 compared to 31.8 for C. This longer length of D was used purposely to check the prediction, based on the results of adiabatic flow interpreted by means of the two-dimensional flow model, that a much longer laminar boundary layer could be maintained, even with heat transfer to the air stream, than was used in test combination C. The results given here for test combination D confirm this prediction quite well.

Test combination D has also been used to measure the velocity profiles for supersonic flow in the test section, with and without heat transfer to the air stream. The preliminary results obtained from velocity profile measurements, discussed in references (2) and (3), confirm that either a laminar boundary layer can exist for the entire tube length, or that transition of this boundary layer to a turbulent one may occur before tube exit. Thus the interpretation of all previous, and present data obtained with this type of apparatus is placed on a secure foundation.

## EXPERIMENTAL RESULTS

Appendix A contains the measurements for flow with heat transfer obtained with test combinations C and D, together with the calculated results based on a simple one-dimensional flow model. In order to keep the size of this paper within reason, only those data which correspond mainly to a laminar boundary layer existing over most of the tube length are given here; the remaining data, corresponding to a boundary layer in transition and to a turbulent boundary layer will be given in similar detail in a later paper of this series. Appendix B contains the analysis for the simple one-dimensional flow model, the detailed method of computation, and a sample calculation.

The number of runs made with test combinations C and D, the ranges of Reynolds numbers covered and the prevailing type of boundary layer present in the tube, are given in Table 2.

TABLE 2

## SUMMARY OF HEAT-TRANSFER TESTS

TEST COMBINATION	TYPE OF BOUNDARY LAYER	NO. OF RUNS	$Re_D$		$Re_L$
			MIN.	MAX.	MAX.
C	Laminar	4	52,000	96,000	2,270,000
C	{ Turbulent Transitional	19	43,000	390,000	8,560,000
D	Laminar	13	22,000	92,000	3,590,000
D	{ Turbulent Transitional	6	20,000	492,000	12,000,000

The diameter Reynolds number is based on the tube diameter and on the mean stream properties measured or computed at the first station — for C the first station is 1.66 in. from the exit plane of the nozzle whereas for D it is 1.19 in. from the exit plane of the nozzle. Hence the inlet diameter Reynolds numbers for C do not correspond exactly to those for D. The length Reynolds number is based on the distance from the end of the curved contour of each nozzle and on the mean stream properties at that distance. Hence the values of  $Re_L$  for C and D are less arbitrary than those for  $Re_D$  and more nearly comparable, especially at a considerable distance downstream from the entrance plane of the tube.

## Laminar Boundary Layer

The data presented here for a laminar boundary layer in a round tube were first interpreted on the basis of a simple one-dimensional flow model. This model ignores completely the growth of the laminar boundary layer in the tube and also the fact that this type of supersonic flow is mainly one of "entrance flow" with insufficient flow length to produce a "fully-developed" flow. Moreover, previous work (5) on adiabatic supersonic flow in a tube has shown that this model is inadequate for calculation of friction coefficients and recovery factors for a laminar boundary layer. In the present paper this simple model is still used since it permits one to get a quick reduction of the original data to useful form, but the computed quantities are interpreted, related, and compared with essentially the correct phenomenological picture of the growth of a laminar boundary layer either on a flat plate or in a tube.

For flow over a flat plate, a laminar boundary layer begins to grow from the leading edge until it undergoes a transition to become a turbulent boundary layer. The transition process occurs in a finite length of flow. The turbulent boundary layer continues to grow in thickness in the direction of flow. This simple picture of plate flow can be used with precision to develop a two-dimensional flow model for supersonic flow in a tube (6). The details of this two-dimensional flow model for tube flow with heat transfer will be given in a later publication. The results obtained with this more exact model justify the method of comparison of tube flow with plate flow which is used in the present paper.

The results computed on the basis of the one-dimensional flow model will also be compared with the theoretical results for tube flow obtained recently in this program (7). These results were obtained by investigation of the basic partial-differential equations of energy, momentum, and continuity for a developing laminar boundary layer adjacent to an isentropic core in the central portion of the tube. After transformations, these equations were solved with the aid of the M.I.T. Differential Analyzer. The solutions were obtained on the basis of the simplifying assumption of constant fluid viscosity and thermal conductivity. The corresponding calculated results will be referred to on the charts to follow as "tube flow, constant  $\mu$  and  $\lambda$ ."

The experimental results for tube flow with a laminar boundary layer, covering the range of inlet diameter Reynolds number from about 20,000 to 100,000, are presented in six charts, Figs. 9 to 14. Each chart shows the measured values of the modified pressure ratio, the wall temperature of the brass test section, the heat flux, and finally the computed values of the Stanton number. Each of these quantities is plotted against the length

Reynolds number. All the data for predominantly laminar boundary layers which were obtained with test combinations C and D are given on these six charts; the remaining data for a predominantly transitional or turbulent boundary layer are given in a later paper and contain only a small amount of information on the laminar boundary layer. Six charts were found to be necessary to present the data in sufficient detail because they were found to be quite sensitive to small changes in values of the inlet diameter Reynolds number.

The ratio of measured local static pressure to stagnation pressure is given in Figs. 9 to 14 in terms of a dimensionless modified pressure ratio mainly to place results from test combinations C and D and runs made with different stagnation temperatures on a comparable basis. The local wall temperature could have been presented in terms of the ratio of local wall temperature to stagnation temperature but the actual variations are too small to warrant use of this ratio. The local heat flux is, in reality, an average value of heat flux over the short length of one of the condensate collecting compartments.

Fig. 9 presents results for the lowest value of the diameter Reynolds number attained in these heat-transfer tests, namely, 22,000. Both runs shown in Fig. 9 were made with test combination D and illustrate the degree of reproducibility of the data for static pressure, wall temperature, and heat flux along the length of the test section. The pressure fluctuations shown in Fig. 9 are not uncommon in this type of experiment. The wall temperature is remarkably constant along the length, with an average deviation from a mean value of less than a fraction of one degree. The heat flux appears to be smooth in the entrance portion of the tube which corresponds to the laminar boundary layer, and then appears to fluctuate about a mean value of 235 Btu/(hr ft<sup>2</sup>).

Fig. 9 compares the computed Stanton number for tube flow with the values predicted for plate flow and for tube flow. The predicted Stanton number for plate flow with zero pressure gradient is taken from Van Driest (8) for a laminar boundary layer with variable viscosity and thermal conductivity; the comparison is made for a free-stream Mach number  $\approx 2.8$  and a ratio of wall temperature to free-stream temperature of 3.0. The predicted Stanton number for tube flow is taken from the theoretical solution given by Toong (7) for a laminar boundary layer with constant viscosity and thermal conductivity. This solution shows that the Stanton number depends both on the length Reynolds number and the diameter Reynolds number so that two lines are shown to cover the range of diameter Reynolds number employed in the tests. For the entrance region of the tube, where a laminar boundary layer is forming, the experimental tube results are in good agreement with the theoretical values for tube flow. The experimental

data lie below the theoretical values for plate flow probably because of the presence of a large adverse pressure gradient in the tube flow.

Fig. 10 shows the results for a diameter Reynolds number of 32,000 for test combination D. The pressure data are smoother and more reproducible than those in Fig. 9, and the heat-flux data cover a much larger range of values than those in Fig. 9. The heat-flux data and the Stanton numbers both indicate a sharp rise in value near the exit of the test section; this sharp rise is one of the first signs noted of transition from a laminar to a turbulent boundary layer in the tube. As in the previous case, where a laminar boundary layer is present, the values of the Stanton number compare well with the theoretical predictions for tube flow but lie below those for plate flow with zero pressure gradient.

Fig. 11 shows the results for 3 runs with test combination D and one run for test combination C. The sensitivity of the data to small changes in diameter Reynolds number is evident in Fig. 11, where the local heat-flux values for Runs B-14 and K-20 are considerably larger than those for Runs B-2 and B-4 even though the diameter Reynolds number is increased only from 45,000 to 51,000. The modified pressure ratio for Run K-20 is slightly smaller than those for the three runs with test combination D, but the same slow rise in pressure with a maximum value attained near the downstream end of the tube is evident in all four runs. Careful study was made of the conditions at this value of the diameter Reynolds number because preliminary data for adiabatic flow had indicated that for this value the laminar boundary layer occupied most of the length of the test section. Substantiation of these preliminary data is seen in runs B-2 and B-4 where a laminar boundary layer was found to exist up to station 17, with a value of length-diameter ratio of 45.3. The agreement of the measured Stanton numbers for tube flow with the theoretical values for plate flow and tube flow is excellent on the basis of the simple one-dimensional flow model. Similar excellent agreement was found in reference (5) for the local apparent friction coefficients of adiabatic tube flow at a diameter Reynolds number of 100,000. Fig. 11 also indicates that the start of the transition from a laminar to a turbulent boundary layer occurs at a value of the length Reynolds number of 900,000 for Run K-20 and about 1,300,000 for the other three runs. These values are in good agreement with those for transition on a flat plate.

In Fig. 9 the value of the Stanton number begins to level off at a length Reynolds number of 200,000, and fluctuations about a constant value extend to a Reynolds number of 800,000. In Fig. 10 a similar behavior is noted between Reynolds numbers of 300,000 and 900,000, and in Fig. 11 between 500,000 and 1,000,000. A possible explanation of this levelling off and fluctuation of values of the Stanton number could be the phenomenon of separation of the laminar boundary layer under the influence of an adverse



pressure gradient which is present over a long length of tube flow. The fluctuations could be partially explained in terms of reattachment of the separated laminar boundary layer. Further work is needed to test this explanation.

Fig. 12 presents the data for a diameter Reynolds number of about 70,000 for 2 runs with test combination D and one run for test combination C. The excellent agreement of the values of the modified pressure ratio and of the heat flux for the laminar boundary layer for the two completely different test combinations indicates the absence of appreciable systematic errors. The second striking feature of the data in Fig. 12 is the steep rise in the heat flux, and likewise in the Stanton number, when the laminar boundary layer undergoes a transition to a turbulent one. The older and shorter test combination C was not long enough to show this feature. The steep rise in heat flux observed here is an excellent indicator of transition. The static pressure, and the wall temperature on the other hand, changed but slightly over the entire eight-diameters of length of this transition process. The values of the measured Stanton numbers in Fig. 12 are in excellent agreement with those predicted for plate flow, and are larger than those for tube flow with a laminar boundary layer. The better agreement with predicted values for plate flow may also be due to the smaller pressure gradient present in the data in Fig. 12 than in Figs. 9, 10, and 11.

Fig. 13 shows the data for a diameter Reynolds number of about 80,000 for Runs B-1 and B-9. The results are similar to those noted for Fig. 12, especially with respect to the steep slope of the curve for heat flux during transition. It should be noted that as the value of the diameter Reynolds number is increased from Fig. 9 on to Fig. 14, the value of the length Reynolds number at transition, computed on the basis of the one-dimensional flow model gradually increased from about 900,000 to about 2,200,000. A similar shift was found in the transition for adiabatic tube flow. The agreement between measured values of the Stanton number and those predicted for plate flow is excellent for this type of measurement in view of published data.

Fig. 14 shows the data for Runs B-7, B-16, K-19, and K-23 for the last and largest value of the diameter Reynolds number, 90,000, which was chosen to demonstrate the data for a predominantly laminar boundary layer. The agreement between the data for the two different test combinations is again excellent. The steep slopes of the curves for heat flux and for Stanton number are again emphasized in the data taken with the longer test combination D. Figs. 13 and 14 indicate smaller values of the adverse pressure gradient than do the preceding figures. For these four runs, the agreement between measured Stanton numbers and plate-flow values for zero pressure gradient is excellent.



## One-Dimensional Flow Model

Previous work (5, 6) has shown that the one-dimensional flow model, 1-DFM, used for the present heat-transfer calculations is not fully adequate for calculation or understanding of adiabatic supersonic flow in the entrance region of a tube. The experimental results given in Figs. 9 to 14, additional data on measured velocity profiles for supersonic tube flow (2, 3), and, finally, unpublished data on measured temperature profiles for supersonic tube flow all show that the simple 1-DFM is not fully adequate to explain the heat-transfer data for supersonic tube flow.

In place of using tube-type flow, as the 1-DFM would suggest, the data have been treated here as though the laminar boundary layer develops in the tube in the same way as a laminar boundary layer develops on a flat plate. A somewhat more complicated flow model, the two-dimensional flow model, 2-DFM, will be used in a subsequent paper to give support to this phenomenological explanation of supersonic tube flow in the entrance region. In addition, this 2-DFM applied to heat-transfer data for tube flow will indicate the means of transforming the tube data for quantitative comparison with heat-transfer data for plate flow. Finally this 2-DFM will be used to show the means of combining all the data for a laminar boundary layer in tube flow so as to reduce the scattering inherent in the measurement of local values of the heat flux over short increments of tube length.

## CONCLUSIONS

Reliable data on heat-transfer coefficients to air flowing at supersonic velocities in a round tube are presented here for the case of a laminar boundary layer. The agreement found between measurements made with completely independent test combinations by different groups of students provides assurance that no significant systematic errors exist.

The data for tube flow are computed on the basis of a simple one-dimensional flow model. Since this model is not fully adequate to explain or interpret the heat-transfer data for supersonic tube flow, these data are interpreted in terms of a laminar boundary layer which begins to grow at tube entrance. The calculated values are compared with the theoretical predictions for a laminar boundary layer developing over a flat plate with zero pressure gradient and with the theoretical predictions for tube flow based on constant viscosity and constant thermal conductivity.

The measured Stanton numbers agree best with the theoretical values for tube flow and deviate most from the values for plate flow for the lowest value of the diameter Reynolds number attained here, namely, 22,000. On the

other hand, the reverse is true at the highest value of the diameter Reynolds number, namely, 90,000. The agreement between measured Stanton numbers and flat-plate values improves as the adverse pressure gradient in the tube decreases, that is, as the value of the diameter Reynolds number increases from 20,000 to 90,000; the agreement at the highest values of the diameter Reynolds number is excellent for this type of measurement.

The transition from a laminar to a turbulent boundary layer for supersonic flow in a tube, with heat transfer is most easily detectable by the sudden sharp rise of the value of heat flux at the transition region, even though hardly any change in static pressure is evident. The numerical value of the length Reynolds number at inception of transition is in excellent agreement with similar published data for a laminar boundary layer on a flat plate.

The data indicate that a fairly great length of supersonic flow can be established in a tube with a laminar boundary layer over most of this length. Hence this type of apparatus represents an inexpensive supersonic wind tunnel for adiabatic and diabatic flow.

The one-dimensional flow model was used in this paper to reduce the experimental values to computed quantities in a simple and quick way. The computed quantities, however, are interpreted, related, and compared with essentially the correct phenomenological picture of the growth of a laminar boundary layer in a tube. The same original data will be treated in a later paper by a more detailed analysis based on a two-dimensional flow model.

#### ACKNOWLEDGMENTS

The results presented here for local coefficients of heat transfer for supersonic flow represent the combined efforts of many graduate students. The assistance of the following men is gratefully acknowledged: A. G. Marcuse, K. K. Klingensmith, J. D. Wyant, W. J. Larkin, W. L. England, G. M. Ketchum, W. O. Young, B. W. Birmingham, L. J. Ingolfstrud, W. S. Wu, and P. Ashurkoff. Mrs. A. B. Walker assisted in some of the computational work. Professor W. H. McAdams contributed to the design of the apparatus in its earlier stages.

This investigation is sponsored as Contract Number N5-ori-07805 by the Office of Naval Research of the United States Navy.

## BIBLIOGRAPHY

1. "Survey of Friction Coefficients, Recovery Factors, and Heat-Transfer Coefficients for Supersonic Flow," by J. Kaye, Journal of the Aeronautical Sciences, Vol. 21, 1954, pp. 117-129.
2. "Experimental Velocity Profiles for Adiabatic Supersonic Flow of Air in a Tube," by J. Kaye, G. A. Brown, and J. J. Dieckmann, Journal of the Aeronautical Sciences, Readers' Forum, Vol. 21, 1954, pp. 203-205.
3. "Experimental Velocity Profiles for Supersonic Flow of Air in a Tube With and Without Heat Transfer," by J. Kaye, G. A. Brown, J. J. Dieckmann, and E. A. Sziklas, to be presented at the Second U. S. National Congress of Applied Mechanics, University of Michigan, June, 1954.
4. "Theoretical Velocity and Temperature Profiles for the Laminar Boundary Layer of the Flow of a Compressible Fluid in the Entrance Region of a Tube," by T. Y. Toong and J. Kaye, to be presented at the Second U. S. National Congress of Applied Mechanics, University of Michigan, June, 1954.
5. "Measurement of Recovery Factors and Friction Coefficients for Supersonic Flow of Air in a Tube; Part I - Apparatus, Data and Results Based on a Simple One-Dimensional Flow Model," by J. Kaye, J. H. Keenan, K. K. Klingensmith, G. M. Ketchum, and T. Y. Toong, Journal of Applied Mechanics, Vol. 19, 1952, pp. 77-96.
6. "Measurement of Recovery Factors and Friction Coefficients for Supersonic Flow of Air in a Tube; Part II - Results Based on a Two-Dimensional Flow Model for Entrance Region," by J. Kaye, T. Y. Toong, and R. H. Shoulberg, Journal of Applied Mechanics, Vol. 19, 1952, pp. 185-194.
7. "The Laminar Boundary Layer of a Steady Compressible Flow in the Entrance Region of a Tube," by T. Y. Toong, Sc.D. Thesis, M.I.T., January 1952.
8. "Investigation of Laminar Boundary Layer in Compressible Fluids Using the Crocco Method," by E. R. Van Driest, NACA Technical Note 2597, January, 1952.
9. "Temperature and Velocity Profiles in the Compressible Laminar Boundary Layer with Arbitrary Distribution of Surface Temperature," by D. R. Chapman and M. W. Rubesin, Journal of the Aeronautical Sciences, Vol. 16, No. 9, pp. 547-565, September 1949.
10. "Gas Tables," by J. H. Keenan and J. Kaye, John Wiley & Sons, New York, New York, 1948.

## APPENDIX A

## MEASUREMENTS AND CALCULATED RESULTS

This appendix contains the detailed dimensions of the two test combinations, the original measurements for diabatic flow, and the calculated results based on the simple one-dimensional flow model. The values of the discharge coefficients for the supersonic nozzles and the properties of air are given in reference (5).

## Details of Nozzles and Test Sections

The values of the nozzle throat diameter  $D^*$ , and the test section diameter  $D$ , are given in Table 3 for the two test combinations.

TABLE 3

## DIAMETERS OF NOZZLES AND TEST SECTIONS

TEST COMBINATION	NOZZLE	TEST SECTION	$D^*$ (in.)	$D$ (in.)
C	Brass	Brass	0.2416	0.502
D	Stainless Steel	Brass	0.2685	0.5018

The length-diameter ratios of the two test sections are given in Table 4. The length is the distance from the end of the curved contour in the supersonic nozzle to the location of the pressure tap of the station in question.

The value of the local heat-transfer area in any collecting compartment is found by multiplying its length by the inner circumference of the test section. For test combination C the length of each collecting compartment for stations 1 through 14 is 1 in., but for the first collecting compartment is 0.656 in. (see Fig. 3). In test combination D the length of the compartments for stations 3 and 18 is 0.75 in., for stations 4 through 9 is 1.00 in., and for stations 10 through 17 is 2.00 in. (see Fig. 6).

## Data and Calculated Results

The original data and calculated results for seventeen runs corresponding to flow with a laminar boundary layer are summarized in Table 5. Thirteen runs were made with combination D and four with combination C. The data include measured values of the stagnation temperature, stagnation

TABLE 4  
DIMENSIONS OF TEST COMBINATIONS C AND D

STATION NO.	C		D	
	L/D	LOCATION OF PRESSURE TAP	L/D	LOCATION OF PRESSURE TAP
1	3.299	Second Compartment	0.1868	Collar
2	5.291	Third	1.619	Test Section Boss
3	7.283	Fourth	2.367	First Compartment
4	9.275	Fifth	4.434	Second
5	11.27	Sixth	6.477	Third
6	13.26	Seventh	8.470	Fourth
7	15.25	Eighth	10.46	Fifth
8	17.24	Ninth	12.46	Sixth
9	19.24	Tenth	14.45	Seventh
10	21.23	Eleventh	17.44	Eighth
11	23.22	Twelfth	21.42	Ninth
12	25.21	Thirteenth	25.41	Tenth
13	27.20	Fourteenth	29.39	Eleventh
14	29.20	Fifteenth	33.38	Twelfth
15			37.37	Thirteenth
16			41.35	Fourteenth
17			45.34	Fifteenth
18			48.08	Sixteenth

pressure, local wall temperature, local static pressure, and local gross and local no-load heat-transfer rates. The calculated results are based on the simple one-dimensional flow model.

Due to experimental difficulties during certain runs, it was occasionally necessary to evaluate certain quantities, such as wall temperature, wall pressure, local heat-transfer rate, by linear interpolation or extrapolation of the remaining data. Such quantities are placed in parentheses in Table 5.

The no-load heat-transfer rates were not determined after every run. For those runs where such data were available, they were averaged and the average values were used also for the runs for which such measurements were omitted.

Inspection of Table 5 shows that heat-transfer parameters are omitted for test combination D at stations 3 and 18. Actually, the net heat-transfer rate measured at station 3 involves the additional heat transfer to the air stream which occurs in the nozzle, collar, and a 0.50-inch length of test section upstream of station 3. Similarly at station 18 the net heat-transfer rate involves additional heat transfer to the air stream in a 0.50-inch length of test section downstream of station 18 and through the downstream boss and end plate to the air in the downstream stagnation tank. The data at these two stations were omitted since they cannot be corrected for these additional heat transfers. The analytical results of Chapman and Rubesin (9), together with measured temperature distributions in the supersonic nozzle, were used to check the measured heat-transfer rates at station 3. The agreement was within the experimental error of the measured heat-transfer rates.

In test combination C, the condensate data at the first compartment,  $q_0$ , were not recorded. The amount of heat transfer to the air stream upstream of station 1 was estimated by linear extrapolation of the data from stations 1 and 2.

TABLE 5  
ORIGINAL DATA AND CALCULATIONS BASED ON ONE-DIMENSIONAL FLOW MODEL

Station No.	P	$T_v$	$\frac{A}{A_0}$	$\frac{A}{A_0}$	$\left(\frac{A}{A_0} \frac{P}{P_0}\right)$	M	$\frac{T_m}{T_0}$	$\left(\frac{P_m}{P_0}\right)^{\frac{1}{\gamma}}$	$\left(\frac{A_m}{A_0}\right)^{\frac{1}{\gamma}}$	h	$\frac{h}{x_m}$	$\frac{h}{x_m}$	$\frac{h}{x_m}$
	psi	$^{\circ}F$	$\frac{Btu}{lb \cdot ft^2}$	$\frac{Btu}{lb \cdot ft^2}$	$\times \sqrt{\frac{T_0}{T_m}}$			$\times 10^{-5}$	$\times 10^{-5}$	hr	$\frac{Btu}{hr \cdot ft^2}$	$\frac{Btu}{hr \cdot ft^2}$	$\frac{Btu}{hr \cdot ft^2}$
Run No. R-16	01	14.933	103.38										
November 2, 1948	1	0.5417	213.50	1243	32	0.1617	2.43	0.4594	0.672	2.22	8.42	46.2	151
	2	0.5640	213.50	670	26	0.1697	2.46	0.4734	0.673	3.44	5.71	30.4	161
	3	0.6019	214.00	731	25	0.1797	2.26	0.4939	0.620	4.57	4.92	25.1	152
$T_r = 79.0^{\circ}F$	4	0.6302	213.99	646	26	0.1920	2.20	0.5090	0.611	5.66	4.36	21.6	200
$P_r = 14.933$ psia	5	0.6610	214.03	551	15	0.1995	2.11	0.5290	0.590	6.65	3.78	18.6	203
	6	0.6906	213.92	539	17	0.2056	2.07	0.5392	0.580	7.69	3.69	17.3	229
	7	0.7193	213.97	534	13	0.2144	2.01	0.5535	0.566	8.64	3.59	16.0	296
$C_v = 0.966$	8	0.7377	213.94	506	24	0.2200	1.97	0.5624	0.558	9.62	3.47	15.1	260
	9	0.7550	213.98	497	32	0.2263	1.94	0.5691	0.551	10.6	3.37	14.7	253
$G = 10.79 \frac{lbm}{sec \cdot ft^2}$	10	0.7719	213.97	481	28	0.2307	1.92	0.5757	0.546	11.6	3.32	14.5	308
	11	0.7829	214.00	474	15	0.2364	1.89	0.5825	0.549	12.7	3.20	14.5	337
	12	0.7903	213.98	515	35	0.2421	1.90	0.5897	0.541	13.7	3.46	15.0	378
	13	0.7903	213.95	510	24	0.2430	1.90	0.5906	0.541	14.7	3.51	15.2	414
	14	0.7669	213.98	551	32	0.2230	1.92	0.5745	0.546	15.9	3.76	16.5	440
of		0.3809	110.72										
Run No. R-19	01	19.626	103.54										
November 16, 1948	1	0.6305	213.51	1360	32	0.1486	2.63	0.4200	0.959	3.16	9.39	50.1	185.12
	2	0.6320	213.51	1042	27	0.1531	2.62	0.4268	0.957	4.26	8.79	40.5	214
	3	0.6520	213.50	890	35	0.1604	2.56	0.4321	0.933	5.79	8.05	35.1	256
$T_r = 73.0^{\circ}F$	4	0.7150	213.41	773	26	0.1611	2.43	0.4573	0.773	7.19	5.30	29.0	269
$P_r = 14.620$ psia	5	0.7453	213.44	691	15	0.1695	2.36	0.4727	0.759	9.07	4.71	25.5	280
	6	0.7591	213.41	627	17	0.1738	2.34	0.4829	0.740	11.2	4.36	22.7	200
$C_v = 0.970$	7	0.7634	213.43	597	43	0.1815	2.25	0.4973	0.719	12.5	4.18	21.1	322
	8	0.8027	213.42	567	34	0.1872	2.20	0.5075	0.704	13.9	3.93	19.9	377
$G = 14.23 \frac{lbm}{sec \cdot ft^2}$	9	0.8466	213.40	560	32	0.1912	2.17	0.5146	0.794	15.3	3.60	17.7	357
	10	0.8645	213.39	567	28	0.1951	2.14	0.5215	0.754	16.7	3.49	16.7	392
	11	0.8764	213.38	590	26	0.1968	2.13	0.5243	0.749	18.1	3.41	19.9	462
	12	0.7604	213.51	586	35	0.1977	2.12	0.5260	0.770	19.6	3.99	19.4	479
	13	0.9069	213.57	522	24	0.2044	2.08	0.5372	0.763	20.8	4.34	20.3	552
	14	0.8779	213.36	754	32	0.1979	2.12	0.5263	0.776	22.7	5.27	25.1	732
of		0.4446	115.35										
Run No. R-20	01	10.863	101.79										
November 16, 1948	1	0.3547	213.51	934	32	0.1465	2.58	0.4281	0.919	1.71	6.49	30.2	126
	2	0.3775	213.50	629	26	0.1599	2.44	0.4550	0.849	2.59	4.39	24.3	120
	3	0.4024	213.55	591	35	0.1624	2.36	0.4736	0.873	3.45	3.93	20.2	145
$T_r = 73.0^{\circ}F$	4	0.4576	213.41	495	26	0.1806	2.19	0.5101	0.840	4.10	3.46	17.1	158
$P_r = 14.050$ psia	5	0.4874	213.54	440	15	0.2009	2.10	0.5312	0.820	4.60	3.11	14.8	167
	6	0.4977	213.55	416	17	0.2050	2.07	0.5383	0.821	5.58	2.95	13.8	183
$C_v = 0.964$	7	0.5142	213.57	414	13	0.2117	2.03	0.5491	0.813	6.30	2.95	13.5	207
	8	0.5430	213.44	375	24	0.2196	1.98	0.5616	0.805	6.93	2.68	12.0	207
$G = 7.814 \frac{lbm}{sec \cdot ft^2}$	9	0.5405	213.53	377	32	0.2250	1.94	0.5710	0.799	7.67	2.70	11.9	229
	10	0.5411	213.57	354	28	0.2264	1.96	0.5661	0.821	8.52	2.55	11.3	241
	11	0.5485	213.66	334	15	0.2279	1.92	0.5744	0.796	9.40	2.77	12.1	243
	12	0.5530	213.54	342	25	0.2304	1.92	0.5755	0.795	10.7	2.77	12.1	255
	13	0.5489	213.52	438	24	0.2300	1.90	0.5705	0.797	10.7	2.99	12.9	351
	14	0.5411	213.51	457	24	0.2321	1.93	0.5800	0.801	11.7	3.33	14.0	431
of		0.2711	122.27										
Run No. R-23	01	19.404	103.17										
November 24, 1948	1	0.6503	212.60	1322	32	0.1527	2.52	0.4410	0.908	3.00	9.07	51.6	170.8
	2	0.6752	212.70	907	26	0.1746	2.47	0.4650	0.870	4.76	6.80	37.3	197.4
	3	0.7025	212.77	625	25	0.1824	2.30	0.4825	0.871	6.14	5.30	32.2	238
$T_r = 73.0^{\circ}F$	4	0.7423	212.79	591	26	0.1912	2.34	0.4779	0.840	7.01	5.57	28.3	262
$P_r = 14.605$ psia	5	0.7795	212.83	506	15	0.1983	2.26	0.4913	0.821	9.25	4.61	24.6	166
	6	0.8152	212.77	637	17	0.1944	2.21	0.4961	0.799	10.6	4.44	22.1	293
$C_v = 0.970$	7	0.8390	212.70	600	13	0.1916	2.17	0.5157	0.785	12.0	4.21	20.5	313
	8	0.8570	212.78	585	34	0.1958	2.14	0.5227	0.776	13.4	3.95	19.0	390
$G = 0.967$	9	0.8779	212.78	578	32	0.2005	2.10	0.5307	0.765	14.7	3.73	18.4	359
	10	0.8639	212.70	559	28	0.2010	2.09	0.5329	0.762	16.2	3.64	18.1	334
$G = 14.07 \frac{lbm}{sec \cdot ft^2}$	11	0.8973	212.80	501	15	0.2048	2.07	0.5379	0.755	17.5	4.16	19.2	445
	12	0.9152	212.75	619	16	0.2028	2.05	0.5445	0.747	18.3	4.24	19.5	493
	13	0.9226	212.71	643	24	0.2104	2.03	0.5572	0.743	20.2	4.75	20.7	545
	14	0.9221	212.79	701	32	0.2036	2.06	0.5358	0.756	22.1	5.47	25.6	740
of		0.5123	116.32										
Run No. R-31	01	14.579	111.19										
September 3, 1952	1	0.6323											
	2	0.6323	212.33	6997	1000	0.1545	2.50	0.4448	0.816	1.93	7.35	38.9	175
$T_r = 83.7^{\circ}F$	3	0.6703	212.40	177	240	0.1857	2.39	0.4674	0.750	3.50	6.01	30.7	199
	4	0.7025	212.73	892	97	0.1752	2.30	0.4825	0.753	4.57	5.57	27.5	245
$P_r = 14.579$ psia	5	0.7477	212.78	978	243	0.1846	2.22	0.5020	0.729	5.67	4.85	25.5	246
	6	0.7669	212.80	681	43	0.1892	2.19	0.5114	0.718	7.51	4.45	22.5	246
$C_v = 0.967$	7	0.7900	212.74	614	52	0.1941	2.14	0.5211	0.707	8.78	4.29	20.4	254
	8	0.8343	212.67	556	56	0.2057	2.07	0.5394	0.698	9.60	3.63	17.6	253
$G = 12.94 \frac{lbm}{sec \cdot ft^2}$	9	0.8920	212.97	558	69	0.2156	1.97	0.5621	0.659	11.5	3.60	15.9	277
	10	0.9458	212.68	430	30	0.2330	1.89	0.5820	0.640	13.7	3.09	13.2	283
	11	0.9709	212.73	440	34	0.2390	1.86	0.5908	0.631	15.0	3.15	13.2	336
	12	1.0170	212.72	393	16	0.2503	1.80	0.6066	0.610	16.1	2.93	12.6	353
	13	1.0074	212.62	414	40	0.2478	1.81	0.6032	0.619	20.7	2.93	12.0	402
	14	1.0074	212.85	403	36	0.2477	1.81	0.6030	0.610	23.1	2.68	11.0	443
	15	0.9689	212.93	326	131	0.2381	1.87	0.5924	0.630	26.1	5.47	23.0	950
	16	0.9170	212.38	1935	153	0.2250	1.94	0.5700	0.646	29.3	14.98	61.7	2797
	17	0.9016	212.00	7768	616	0.2200	1.97	0.5633	0.650	31.2			
of		0.6804	115.28										

TABLE 5 - Continued

Station No.	P	T <sub>v</sub>	$\frac{1}{A}$	$\frac{1}{A}$	$\left(\frac{A \cdot P}{c_p \cdot P_{01}}\right)$	M	$\frac{T}{T_{01}}$	(Re <sub>D</sub> )	(2r <sub>L</sub> )	h	$\frac{h}{A_b}$	$\frac{h}{A_w}$	$\left(\frac{h}{c_p \cdot C}\right)$	
	psia	°F	Grains	lb	lb			x10 <sup>-5</sup>	x10 <sup>-5</sup>				x10 <sup>4</sup>	
			lbm	hr <sup>2</sup>	hr <sup>2</sup>	$\sqrt{\frac{c_p}{T_{01}}}$				$\frac{h}{hr \cdot ft^2 \cdot C}$				
Run No. B-2	01	0.795	109.9											
1	0.4269													
September 3, 1952	2	0.4263												
3	0.4278	212.54	5192	1059	0.1768	2.29	0.4207	0.450	1.06					
T <sub>r</sub> = 32.5 °F	4	0.4044	211.38	1002	340	0.1916	2.17	0.4154	1.48	5.01	24.2	108	7.48	
5	0.5092	212.87	600	97	0.2074	2.05	0.4022	0.409	2.65	1.79	17.4	113	5.67	
P <sub>r</sub> = 14.524 psia	6	0.5413	212.75	705	243	0.2251	1.95	0.5672	0.393	3.33	15.4	130	5.23	
7	0.5782	213.03	441	43	0.2349	1.80	0.5049	0.362	4.00	3.02	12.9	135	4.52	
c <sub>v</sub> = 0.952	8	0.6125	212.19	319	50	0.2523	1.79	0.4993	0.369	4.60	2.51	10.3	128	
9	0.6472	212.70	374	56	0.2664	1.72	0.6200	0.360	5.19	2.43	9.67	140	3.67	
G = 7.747 $\frac{lbm}{sec \cdot ft^2}$	10	0.6856	212.96	378	89	0.2822	1.65	0.6474	0.350	6.11	2.26	8.72	152	
11	0.7145	212.81	324	30	0.2938	1.60	0.6611	0.344	7.26	2.26	8.99	191	3.53	
12	0.7357	212.83	349	34	0.3024	1.57	0.7036	0.339	8.62	2.44	9.11	231	3.65	
13	0.7915	212.96	290	16	0.3251	1.48	0.6944	0.330	9.70	2.34	7.71	227	3.19	
14	0.7624	212.69	299	40	0.3154	1.52	0.6945	0.333	11.1	2.03	7.41	247	3.03	
15	0.7721	212.90	302	35	0.3160	1.51	0.6960	0.332	12.4	2.09	7.62	285	3.13	
16	0.7911	213.06	411	131	0.3206	1.50	0.6999	0.330	13.7	2.21	8.00	321	3.31	
17	0.7337	212.85	409	153	0.3007	1.57	0.6687	0.338	15.3	2.67	9.92	450	3.99	
18	(0.7007)	(212.70)	323	616	0.2960	1.63	0.6520	0.345	16.6					
of	1.5225	136.33												
Run No. P-3	01	12.039	111.66											
1	0.5713													
September 4, 1952	2	0.5637												
3	0.5715	212.66	5053	724	0.1619	2.42	0.4597	0.696	1.65					
T <sub>r</sub> = 30.0 °F	4	0.6117	212.64	1247	340	0.1720	2.33	0.4795	0.660	3.00	6.86	25.4	159	
5	0.6806	213.10	729	96	0.1900	2.06	0.4944	0.649	4.21	5.33	26.7	172	5.43	
P <sub>r</sub> = 14.763 psia	6	0.6877	213.30	525	243	0.1934	2.15	0.5115	0.622	5.77	4.40	21.0	175	
7	0.7170	213.25	670	58	0.2018	2.10	0.5233	0.608	6.36	3.90	18.2	190	3.50	
c <sub>v</sub> = 0.963	8	0.7211	213.47	420	62	0.2051	2.07	0.5305	0.601	7.49	3.59	16.1	201	
9	0.7753	213.09	404	60	0.2175	1.99	0.5813	0.582	8.41	3.26	14.5	209	3.32	
G = 11.36 $\frac{lbm}{sec \cdot ft^2}$	10	0.7543	213.37	426	59	0.2309	1.91	0.5750	0.564	9.84	3.05	13.1	226	
11	0.7715	213.11	407	29	0.2442	1.83	0.5902	0.540	11.7	2.92	12.1	260	2.96	
12	0.8020	213.15	301	18	0.2522	1.79	0.6106	0.510	13.7	2.67	10.8	275	2.72	
13	0.8438	213.14	354	22	0.2575	1.73	0.6267	0.526	15.5	2.69	10.7	314	2.74	
14	0.8428	213.08	394	44	0.2652	1.75	0.6221	0.510	17.5	2.71	10.8	356	2.76	
15	0.9436	213.00	383	30	0.2786	1.74	0.6230	0.520	19.7	2.73	10.8	405	2.78	
16	0.9357	213.10	572	130	0.2694	1.78	0.6220	0.541	22.0	2.80	10.9	457	3.00	
17	0.8715	213.01	1156	190	0.2484	1.84	0.5910	0.546	24.7	3.05	11.6	512	3.20	
18	(0.8525)	(212.95)	6163	992	0.2302	1.91	0.5775	0.559	26.9					
of	0.7000	135.16												
Run No. B-4	01	8.927	109.79											
1	0.4263													
September 4, 1952	2	0.4220												
3	0.4245	212.74	5114	994	0.1720	2.32	0.4211	0.463	1.10					
T <sub>r</sub> = 32.0 °F	4	0.4416	212.55	1036	340	0.1796	2.26	0.4930	0.451	2.62	5.23	26.3	110	
5	0.5092	213.19	579	26	0.2069	2.06	0.5414	0.416	2.69	1.69	17.0	110	5.44	
P <sub>r</sub> = 14.756 psia	6	0.5330	213.29	660	243	0.2105	1.99	0.5600	0.403	3.42	1.14	14.0	118	
7	0.5765	213.35	437	50	0.2340	1.89	0.5836	0.369	4.17	2.07	12.3	128	4.22	
c <sub>v</sub> = 0.959	8	0.5504	212.13	394	62	0.2351	1.80	0.5057	0.362	4.73	2.53	10.8	134	
G = 7.765 $\frac{lbm}{sec \cdot ft^2}$	9	0.5911	213.13	397	84	0.2573	1.77	0.6156	0.371	7.56	2.32	9.26	155	
10	0.6920	213.09	331	29	0.2684	1.69	0.6360	0.361	6.29	2.35	9.24	161	3.47	
11	0.7547	213.14	332	35	0.2754	1.64	0.6473	0.356	7.63	2.32	8.98	192	3.42	
12	0.7649	212.50	779	22	0.3112	1.53	0.6001	0.340	10.0	2.01	7.39	217	2.96	
13	0.7593	213.25	203	34	0.3072	1.55	0.6750	0.342	11.4	1.96	6.84	230	2.74	
14	0.7776	213.22	250	36	0.3148	1.52	0.6940	0.332	12.6	1.97	6.60	227	2.70	
15	0.7625	212.95	300	430	0.3100	1.54	0.6797	0.340	14.0	2.03	7.44	268	2.99	
16	0.7497	213.13	460	198	0.3028	1.57	0.6711	0.343	15.5	2.06	7.66	347	3.04	
17	(0.7365)	(213.25)	3220	992	0.2972	1.59	0.6640	0.345	16.6					
of	0.5300	137.21												
Run No. B-5	01	6.408	107.15											
1	0.3120													
October 3, 1952	2	0.3066												
3	0.3314	212.36	5467	995	0.1862	2.21	0.5050	0.322	0.762					
T <sub>r</sub> = 71.0 °F	4	0.3492	212.51	948	340	0.1963	2.14	0.4757	0.312	1.40	4.58	21.6	97.0	
5	(0.4030)	212.57	636	86	0.2263	1.93	0.5770	0.286	1.86	4.12	10.0	117	8.37	
P <sub>r</sub> = 14.597 psia	6	0.4595	213.01	624	243	0.2567	1.77	0.6153	0.270	2.29	3.31	13.5	114	
7	0.4910	213.15	355	58	0.2748	1.68	0.6304	0.262	2.74	2.25	8.82	92.3	5.61	
c <sub>v</sub> = 0.955	8	0.5127	212.63	424	62	0.2868	1.63	0.6529	0.257	3.00	2.76	10.6	132	
9	0.5267	212.66	323	60	0.2945	1.60	0.6618	0.253	3.66	2.61	7.62	110	4.08	
G = 5.706 $\frac{lbm}{sec \cdot ft^2}$	10	0.5577	213.11	349	69	0.3116	1.53	0.6006	0.247	4.31	1.99	7.33	128	4.04
11	0.5770	212.97	310	29	0.3227	1.49	0.6920	0.244	5.22	2.17	7.87	169	4.11	
12	0.6073	212.97	299	30	0.3389	1.44	0.7078	0.239	6.07	2.02	7.17	182	4.11	
13	0.6212	212.66	323	22	0.3464	1.41	0.7140	0.237	6.96	2.36	3.28	243	4.79	
14	0.6305	213.07	375	30	0.3513	1.40	0.7192	0.235	7.55	2.21	7.10	257	4.49	
15	0.6657	213.06	341	36	0.3377	1.44	0.7062	0.241	8.91	2.41	8.73	212	4.90	
16	0.6463	212.43	422	130	0.3472	1.41	0.7355	0.236	9.74	2.80	9.77	404	5.69	
17	0.6626	212.00	594	190	0.3348	1.45	0.7348	0.236	10.8	3.19	11.3	511	6.47	
18	(0.5777)	(213.04)	3296	992	0.3259	1.48	0.6952	0.240	11.5					
of	0.3733	135.24												



TABLE 2 - Continued

Station No.	P	$t_f$	$\frac{A}{A_n}$	$\frac{1}{n}$	$\left(\frac{A}{A_n}\right)^2 \frac{P}{P_0}$	M	$\frac{T}{T_0}$	$(\mu_0)$	$(\mu_1)$	n	$\frac{hD}{A_m}$	$\frac{hL}{A_m}$	$\left(\frac{h}{c_p}\right)$
	psia	$^{\circ}F$	Gross lbs. area $\frac{Btu}{hr-ft^2}$	$\frac{Btu}{hr-ft^2}$	$\frac{P}{P_0}$			$\times 10^{-5}$	$\times 10^{-5}$		$\frac{Btu}{hr-ft^2}$		$\times 10^4$
Run No. B-7													
1	16.003	110.09											
2	0.7415												
October 6, 1952													
3	0.7415												
4	0.7415												
5	(0.820)	213.77	7402	1201	0.1603	2.44	0.4565	0.225	2.47	8.61	44.9	201	6.72
6	0.820	213.31	1497	346	0.1698	2.35	0.4752	0.081	3.95	6.13	31.0	201	4.78
7	0.820	213.47	903	86	0.1772	2.22	0.5030	0.036	7.08	6.16	30.4	201	4.01
8	0.820	213.03	1103	232	0.1846	2.17	0.5159	0.017	8.55	5.12	24.6	251	4.02
9	0.820	213.03	736	56	0.1912	2.12	0.5272	0.011	9.98	4.71	22.1	276	3.67
10	0.820	213.59	613	108	0.2054	2.07	0.5379	0.011	11.3	3.83	17.6	325	2.99
11	0.820	213.05	648	130	0.2143	2.01	0.5524	0.011	13.4	3.03	17.6	308	3.07
12	0.820	213.63	609	45	0.2259	1.94	0.5714	0.011	16.0	3.55	15.4	331	2.77
13	0.820	213.72	460	47	0.2321	1.90	0.5807	0.011	18.7	3.17	13.5	343	2.47
14	0.820	213.68	450	27	0.2453	1.83	0.5954	0.011	21.4	3.26	13.8	402	2.54
15	0.820	213.75	230	62	0.2640	1.83	0.5976	0.011	23.5	3.67	15.2	508	2.86
16	0.820	213.75	144	36	0.2847	1.80	0.5945	0.011	27.2	4.72	20.0	747	3.60
17	0.820	213.75	144	163	0.2847	1.80	0.5945	0.011	30.9	12.99	50.0	747	14.13
18	0.820	213.69	3308	225	0.2222	1.96	0.6658	0.011	33.7	24.90	100	4896	19.43
or	0.7744	132.50	9744	1087	0.2220	1.96	0.6654	0.011	33.7	24.90	100	4896	19.43
Run No. B-9													
1	14.571	106.01											
2	0.6273												
November 14, 1952													
3	0.6273												
4	0.6273												
5	(0.723)	210.36	6352	870	0.1614	2.43	0.4500	0.003	1.90	0.07	4.0	120.4	7.30
6	0.723	210.34	1438	327	0.1693	2.35	0.4743	0.003	3.49	0.07	4.0	120.4	4.73
7	0.723	210.93	813	70	0.1794	2.27	0.4922	0.003	4.87	0.07	4.0	120.4	4.03
8	0.723	210.17	970	590	0.1872	2.19	0.5093	0.003	6.17	0.07	4.0	120.4	3.59
9	0.723	210.22	697	65	0.1904	2.18	0.5134	0.003	7.57	0.07	4.0	120.4	3.59
10	0.723	210.14	636	54	0.1955	2.13	0.5246	0.003	8.94	0.07	4.0	120.4	3.59
11	0.723	210.97	549	62	0.2046	2.07	0.5375	0.003	10.0	0.07	4.0	120.4	3.59
12	0.723	210.77	513	69	0.2117	2.07	0.5503	0.003	11.7	0.07	4.0	120.4	3.59
13	0.723	210.65	457	29	0.2214	1.92	0.5747	0.003	14.0	0.07	4.0	120.4	3.59
14	0.723	210.14	461	30	0.2312	1.87	0.5991	0.003	16.0	0.07	4.0	120.4	3.59
15	0.723	210.65	419	21	0.2410	1.82	0.6235	0.003	18.0	0.07	4.0	120.4	3.59
16	0.723	210.10	406	55	0.2508	1.77	0.6479	0.003	20.0	0.07	4.0	120.4	3.59
17	0.723	210.17	437	54	0.2606	1.72	0.6723	0.003	22.0	0.07	4.0	120.4	3.59
18	0.723	210.17	437	54	0.2704	1.67	0.6967	0.003	24.0	0.07	4.0	120.4	3.59
19	0.723	210.17	437	54	0.2802	1.62	0.7211	0.003	26.0	0.07	4.0	120.4	3.59
20	0.723	210.17	437	54	0.2900	1.57	0.7455	0.003	28.0	0.07	4.0	120.4	3.59
or	0.5792	130.74	1438	1438	0.1610	2.43	0.4500	0.003	30.2	0.07	4.0	120.4	3.59
Run No. B-10													
1	4.539	104.10											
2	0.1792												
December 11, 1952													
3	0.1792												
4	0.1792												
5	(0.257)	211.73	4260	306	0.1904	2.13	0.5237	0.019	0.518	0.00	12.0	57.4	7.39
6	0.257	211.89	475	4	0.2021	1.90	0.5600	0.019	0.914	0.00	12.0	57.4	7.39
7	0.257	211.76	376	50	0.2107	1.91	0.5706	0.019	1.29	0.00	12.0	57.4	7.39
8	0.257	210.19	326	34	0.2192	1.90	0.5811	0.019	1.66	0.00	12.0	57.4	7.39
9	0.257	210.23	224	26	0.2277	1.87	0.5920	0.019	2.04	0.00	12.0	57.4	7.39
10	0.257	210.12	250	25	0.2362	1.83	0.6029	0.019	2.41	0.00	12.0	57.4	7.39
11	0.257	210.00	313	52	0.2447	1.84	0.6138	0.019	2.79	0.00	12.0	57.4	7.39
12	0.257	210.15	259	21	0.2532	1.84	0.6247	0.019	3.16	0.00	12.0	57.4	7.39
13	0.257	210.22	279	16	0.2617	1.80	0.6356	0.019	3.54	0.00	12.0	57.4	7.39
14	0.257	210.08	306	28	0.2702	1.77	0.6465	0.019	3.92	0.00	12.0	57.4	7.39
15	0.257	211.79	267	27	0.2787	1.75	0.6574	0.019	4.30	0.00	12.0	57.4	7.39
16	0.257	211.77	207	51	0.2872	1.72	0.6683	0.019	4.68	0.00	12.0	57.4	7.39
17	0.257	210.11	259	33	0.2957	1.69	0.6792	0.019	5.06	0.00	12.0	57.4	7.39
18	0.257	210.15	203	33	0.3042	1.67	0.6901	0.019	5.44	0.00	12.0	57.4	7.39
19	0.257	210.06	196	37	0.3127	1.65	0.7010	0.019	5.82	0.00	12.0	57.4	7.39
20	0.257	210.06	196	37	0.3212	1.63	0.7119	0.019	6.20	0.00	12.0	57.4	7.39
or	0.1992	139.50	2575	873	0.1902	2.13	0.5237	0.019	7.74	0.00	12.0	57.4	7.39
Run No. B-11													
1	4.560	100.74											
2	0.2534												
December 12, 1952													
3	0.2534												
4	0.2534												
5	(0.3252)	211.10	3921	619	0.1950	2.14	0.5212	0.022	0.504	0.00	11.78	50.6	7.03
6	0.3252	211.05	412	77	0.2034	2.04	0.5455	0.022	0.951	0.00	11.78	50.6	6.54
7	0.3252	211.27	356	49	0.2118	1.95	0.5698	0.022	1.39	0.00	11.78	50.6	6.05
8	0.3252	211.00	305	28	0.2202	1.87	0.5941	0.022	1.83	0.00	11.78	50.6	5.56
9	0.3252	210.99	299	37	0.2286	1.83	0.6184	0.022	2.27	0.00	11.78	50.6	5.07
10	0.3252	211.78	160	51	0.2370	1.79	0.6427	0.022	2.71	0.00	11.78	50.6	4.58
11	0.3252	211.90	257	19	0.2454	1.75	0.6670	0.022	3.15	0.00	11.78	50.6	4.09
12	0.3252	211.74	276	21	0.2538	1.71	0.6913	0.022	3.59	0.00	11.78	50.6	3.60
13	0.3252	211.70	276	33	0.2622	1.67	0.7156	0.022	4.03	0.00	11.78	50.6	3.11
14	0.3252	211.67	256	24	0.2706	1.63	0.7399	0.022	4.47	0.00	11.78	50.6	2.62
15	0.3252	211.71	266	25	0.2790	1.60	0.7642	0.022	4.91	0.00	11.78	50.6	2.13
16	0.3252	211.71	266	32	0.2874	1.56	0.7885	0.022	5.35	0.00	11.78	50.6	1.64
17	0.3252	211.79	266	33	0.2958	1.52	0.8128	0.022	5.79	0.00	11.78	50.6	1.15
18	0.3252	211.75	2284	751	0.1950	2.14	0.5212	0.022	6.23	0.00	11.78	50.6	0.66
or	0.2104	160.14			0.1950	2.14	0.5212	0.022	7.78	0.00	11.78	50.6	0.17

[illegible]

## APPENDIX B

## ANALYSIS AND SAMPLE CALCULATION

## Analysis

Consider the steady flow of air from a stagnation state through a supersonic nozzle and then through a round tube of constant cross-sectional area in which heat is added to the air stream. The following assumptions are made in the analysis:

1. The flow is one-dimensional, i.e. all fluid properties are uniform at any cross section.
2. Air is a perfect gas with a constant value of the ratio of specific heats ( $k = 1.40$ ) over the range of temperature under consideration.
3. Heat added to the air stream is measured by the amount of condensate collected in the various compartments.

The following relations hold at each section in the tube:

$$\text{Continuity:} \quad w = \rho VA \quad (1)$$

$$\text{Equation of State:} \quad p = \rho RT \quad (2)$$

$$\text{Energy:} \quad c_p T_{oi} = c_p T + V^2/2g \quad (3)$$

$$\text{Definition:} \quad M^2 = V^2/gkRT \quad (4)$$

The discharge coefficient of the supersonic nozzle is defined by

$$c_w = (w/A^*)/(w/A^*)_s \quad (5)$$

For isentropic flow to the nozzle throat

$$G_s^* = (w/A^*)_s = \sqrt{\frac{gk}{R} \frac{k+1}{2}} \frac{p^*}{\sqrt{T_{oi}}} \quad (6)$$

$$p^*/p_{oi} = \left(\frac{k+1}{2}\right)^{\frac{k}{1-k}} \quad (7)$$

For a control volume which encloses the fluid between the upstream stagnation state and the section at the center of the measuring compartment of station  $j$ , the energy equation becomes for test combination C:

$$q_j/2 + \sum_{n=0}^{n=j-1} q_n = c_p (T_{oj} - T_{oi}). \quad (8a)$$

For test combination D the energy equation is:

$$q_j/2 + \sum_{n=3}^{n=j-1} q_n = c_p (T_{oj} - T_{oi}). \quad (8b)$$

Combining Equations (1) through (7),

$$\frac{1}{c_w} \frac{p}{p_{oi}} \frac{A}{A^*} \sqrt{\frac{T_{oi}}{T_{oj}}} = \left( \frac{2}{k+1} \right)^{\frac{k+1}{2(k-1)}} \frac{1}{M \sqrt{1 + \frac{k-1}{2} M^2}} = f_1(M, k). \quad (9)$$

The right-hand side of Equation (9) is a unique function of the Mach number if  $k$  is constant. This function is tabulated under the heading  $pA/p_o A^*$  in Table 30 of reference (10). The symbol  $p_o$  of reference (10) is identical with  $p_{oi}$  used here.

All the quantities on the left-hand side of Equation (9) are measured except  $c_w$  and  $T_{oj}$ . Equation (8) permits the calculation of  $T_{oj}$  from measured data. The plot of  $c_w$  versus  $(Re^*)_{D_s}$ , given in reference (5), where

$$(Re^*)_{D_s} \equiv G_s^* D_s / \mu^* \quad (10)$$

was used. Note that  $G_s^*$  can be found from Equations (6) and (8) from measured data and that  $\mu^*$  can be found from the temperature.

$$T^* = 0.83333 T_{oi} = 0.83333 (t_{oi} + 459.69). \quad (11)$$

With the Mach number known, the mean-stream temperature can be found from

$$T_m / T_{oj} = 1 / (1 + \frac{k-1}{2} M^2) \quad (12)$$

which is tabulated in Table 30 of reference (10) as  $T/T_o$ . The following equations were used to complete the calculations:

$$G = c_w G_s^* A^*/A \quad (13)$$

$$Re_D = GD/\mu_m \quad (14)$$

$$Re_L = GL/\mu_m = Re_D(L/D) \quad (15)$$

$$h = q/A'(T_w - T_{aw}) \quad (16)$$

$$Nu_D = hD/\lambda_m \quad (17)$$

$$Nu_L = hL/\lambda_m = Nu_D(L/D) \quad (18)$$

$$St = h/c_p G \quad (19)$$

In order to calculate the local heat-transfer coefficient from Equation (16), it is necessary to calculate the adiabatic-wall temperature  $T_{aw}$ . For this calculation  $T_{aw}$  was found from

$$r = \frac{T_{aw} - T_m}{T_{oi} - T_m} \quad (20)$$

In order to calculate the local heat-transfer coefficients from Equation (16), the adiabatic-wall temperature can be calculated from the recovery factors for adiabatic tube flow given in reference (5). Since the original data on which these recovery factors are based were also available in the form of the ratio of adiabatic-wall temperature to stagnation temperature, these original data for a laminar boundary layer were plotted and then averaged. An average value of  $(T_{aw}/T_{oi})$  of 0.940 was used in this paper in order to reduce the time required for these computations.

### Sample Calculation

A sample calculation of Run No. B-7 is given in Table 6. The calculations and equation numbers given in the headings refer to the preceding analysis. The values given in Tables 5 and 6 are based on calculations made with five or six significant figures throughout.



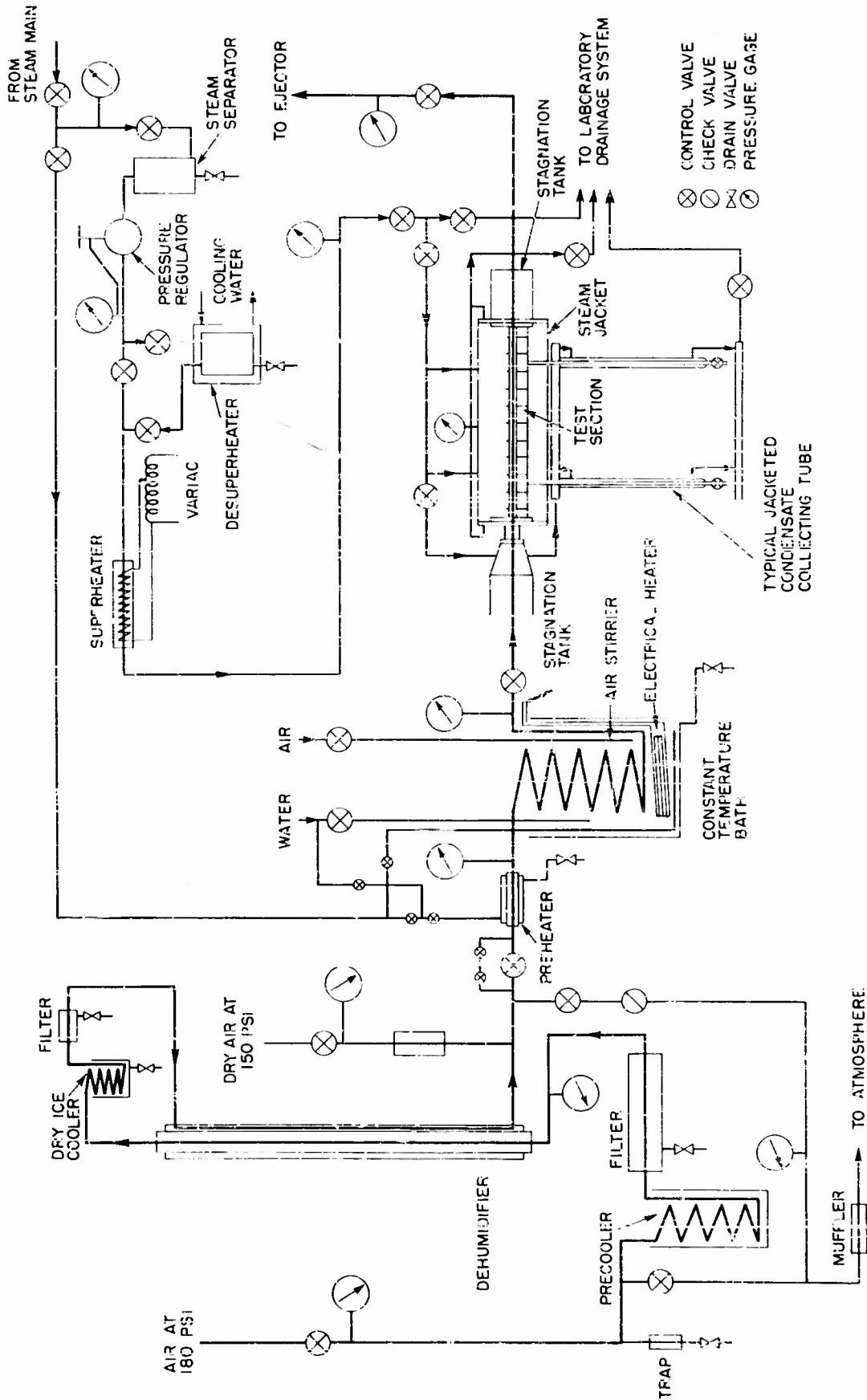
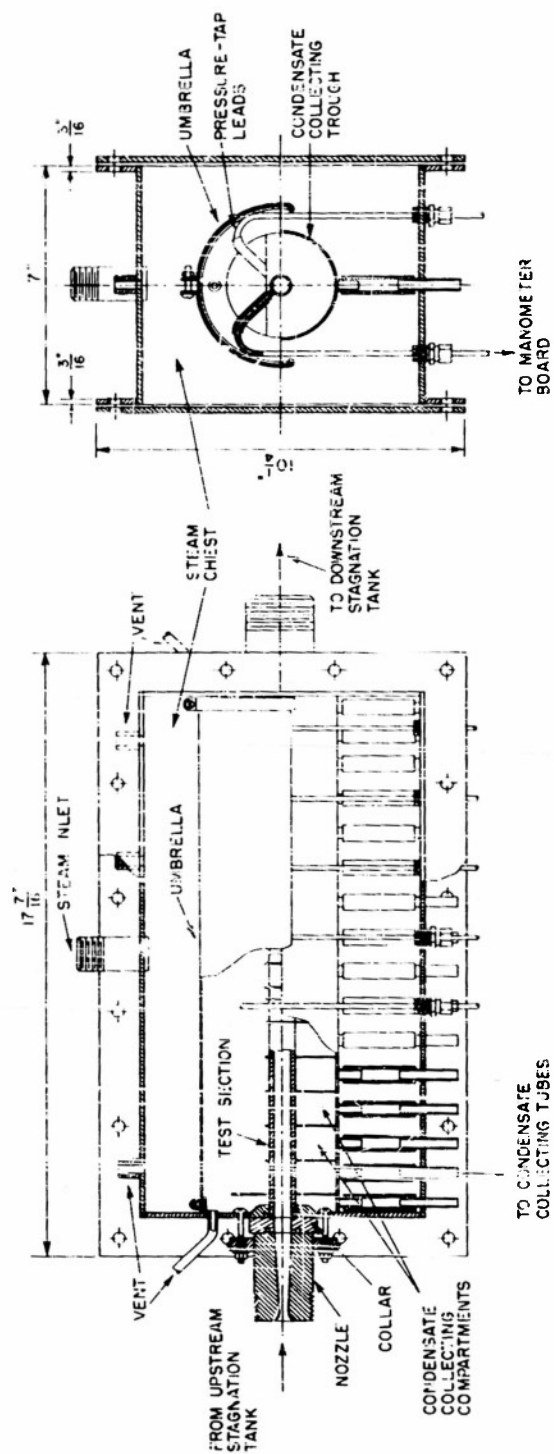
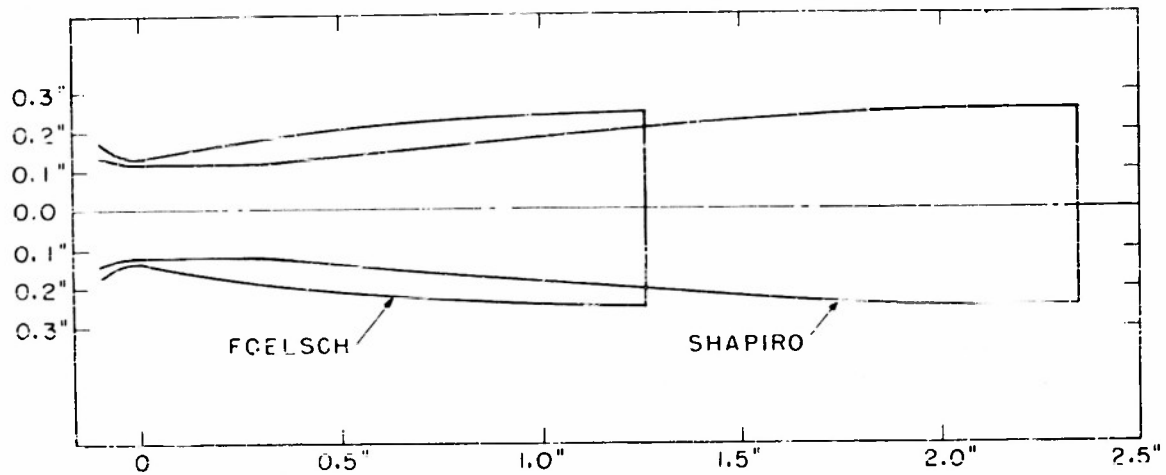


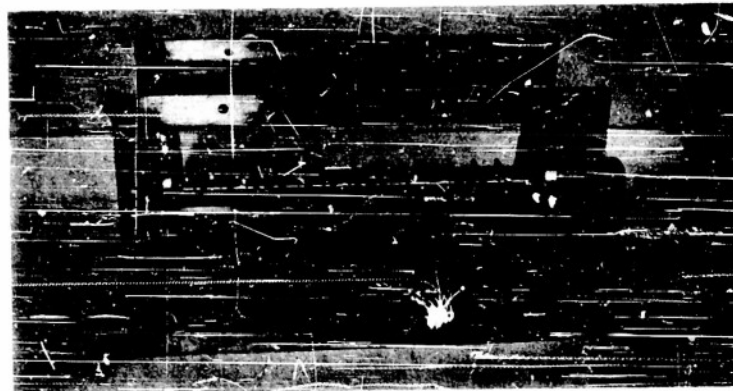
FIG 1 SCHEMATIC LAYOUT OF TEST COMBINATIONS C AND D



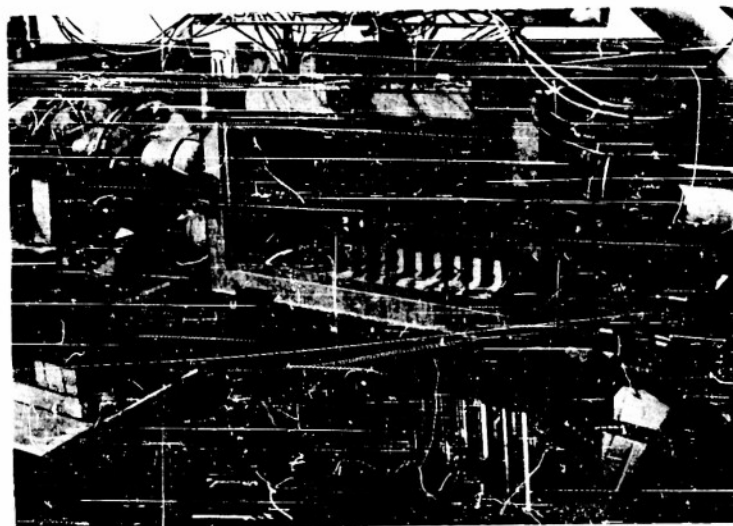




COMPARISON OF SUPERSONIC NOZZLES  
FIG. 2



TEST COMBINATION C, BEFORE ASSEMBLY  
FIG. 4



TEST COMBINATION C, AFTER ASSEMBLY  
FIG. 5

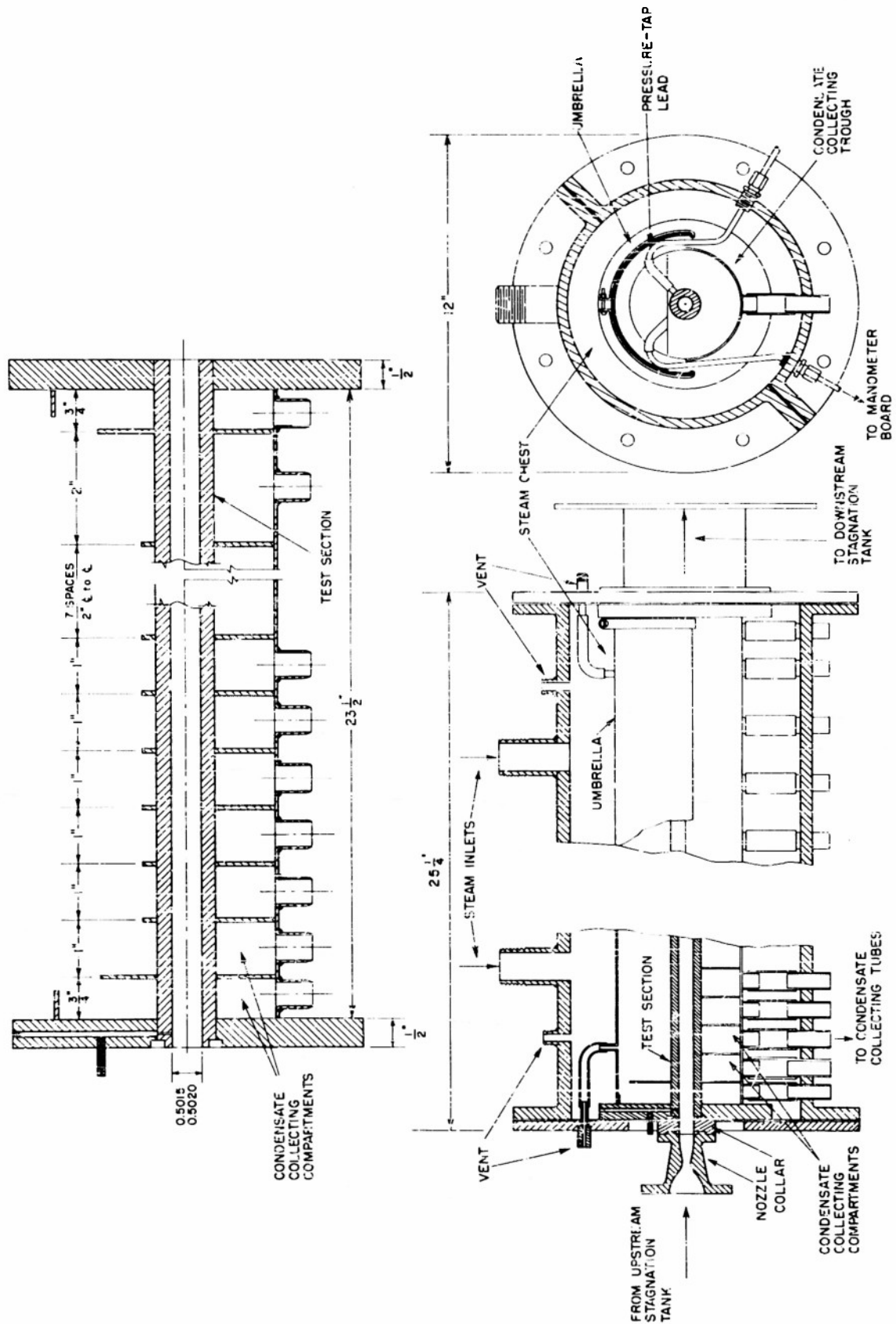
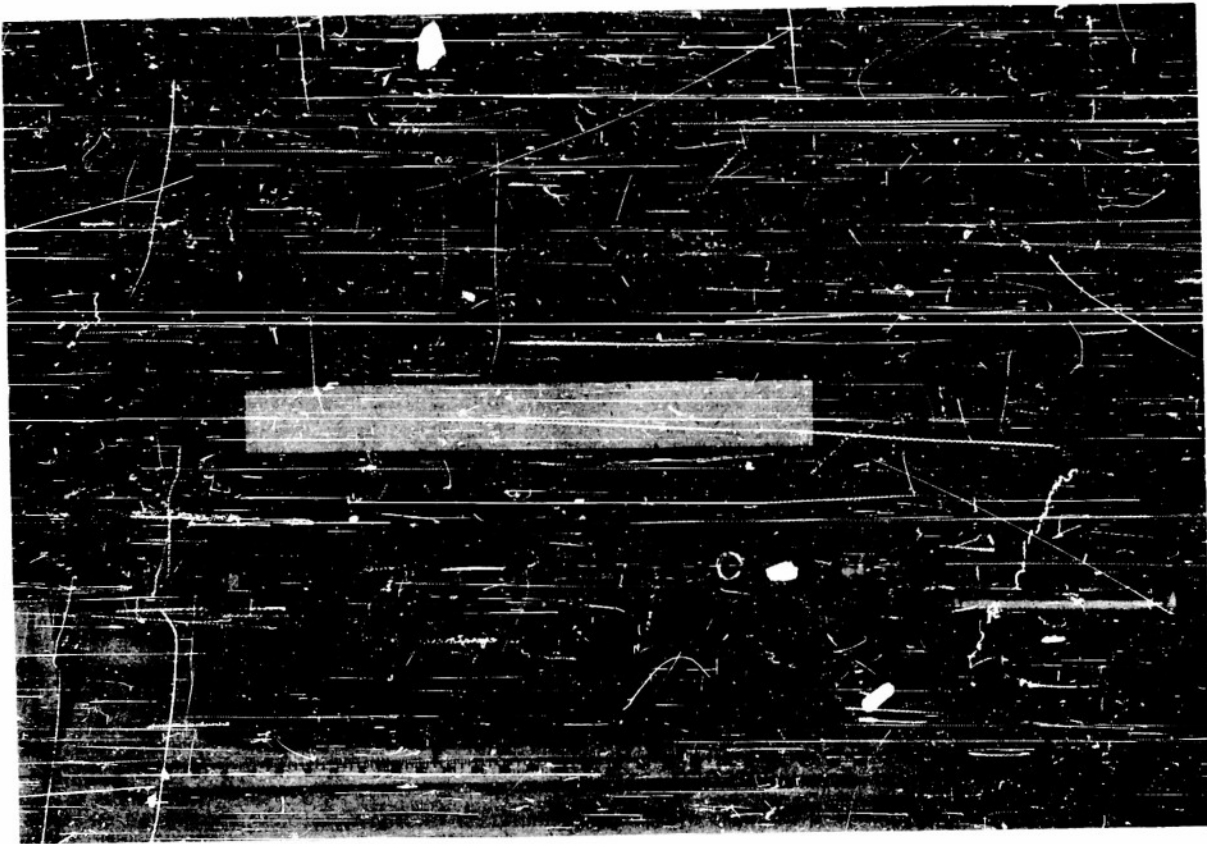
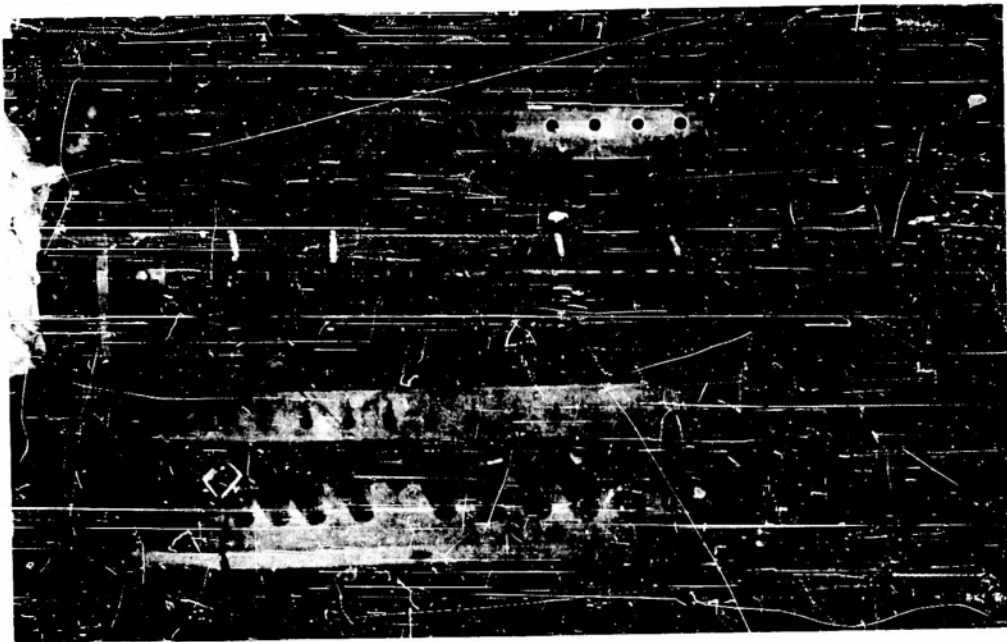


FIG. 6 DETAILS OF TEST COMBINATION D



TEST COMBINATION D, BEFORE ASSEMBLY

FIG. 7



TEST COMBINATION D, AFTER ASSEMBLY

FIG. 8

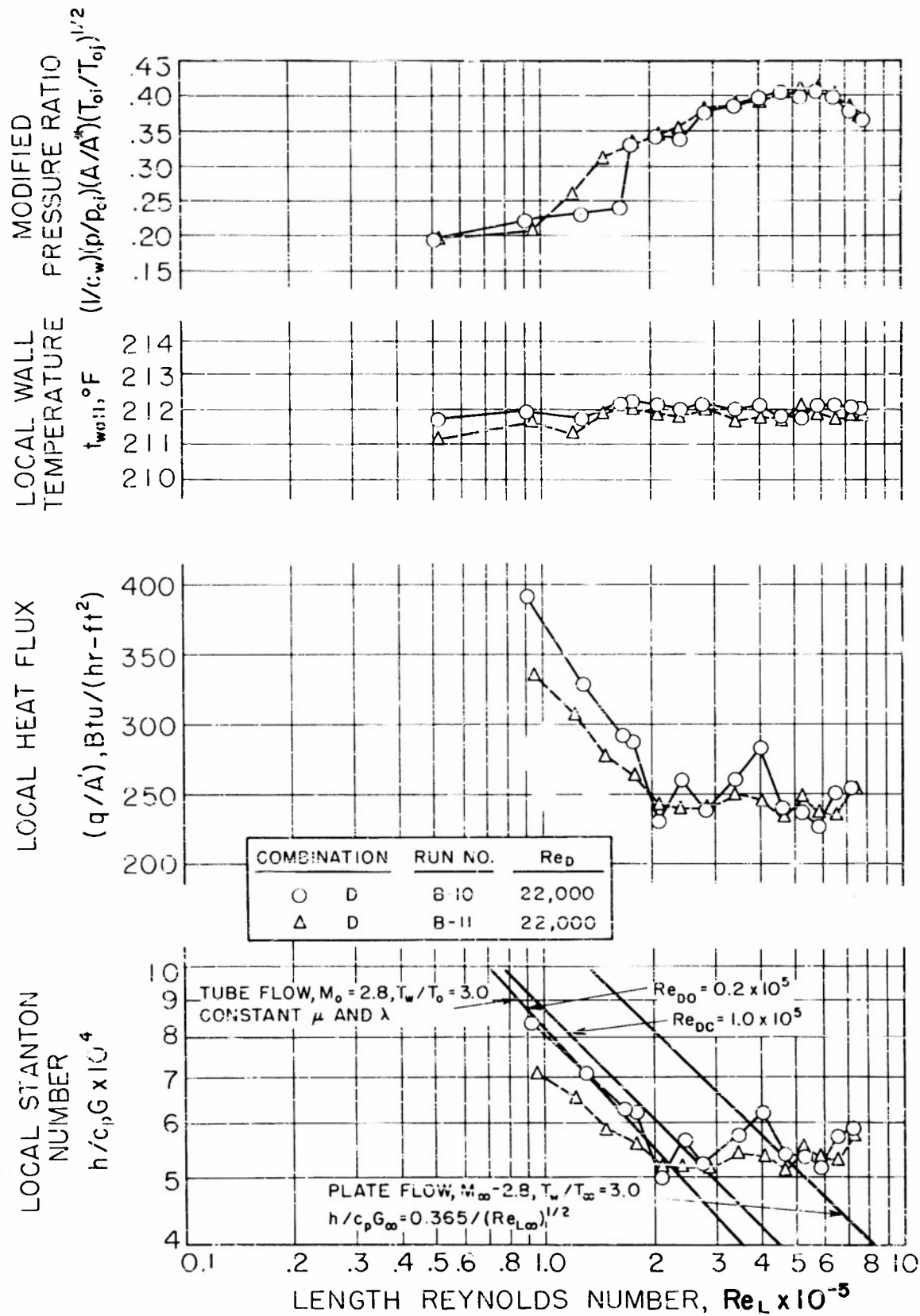


FIGURE 9

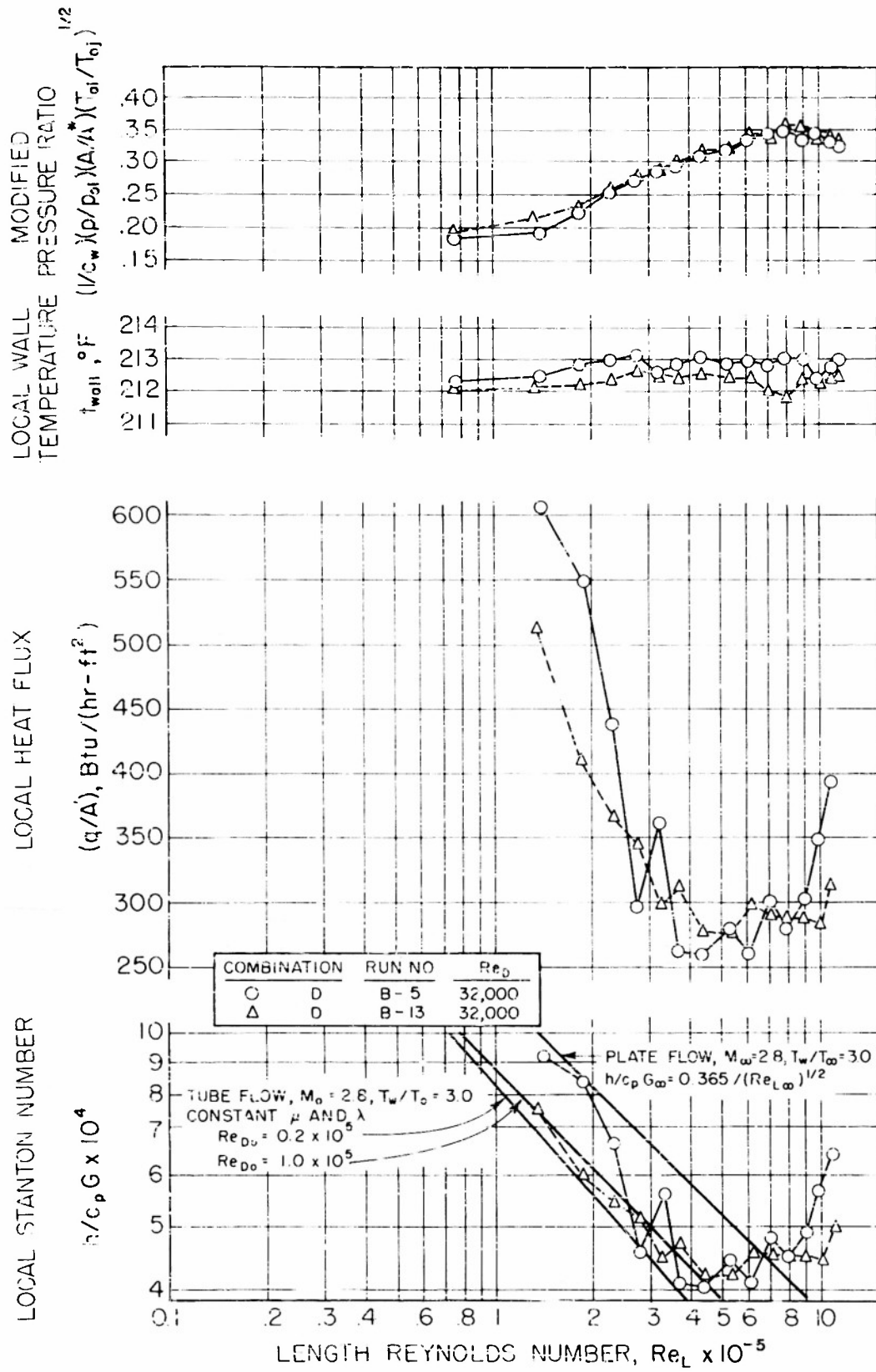


FIGURE 10

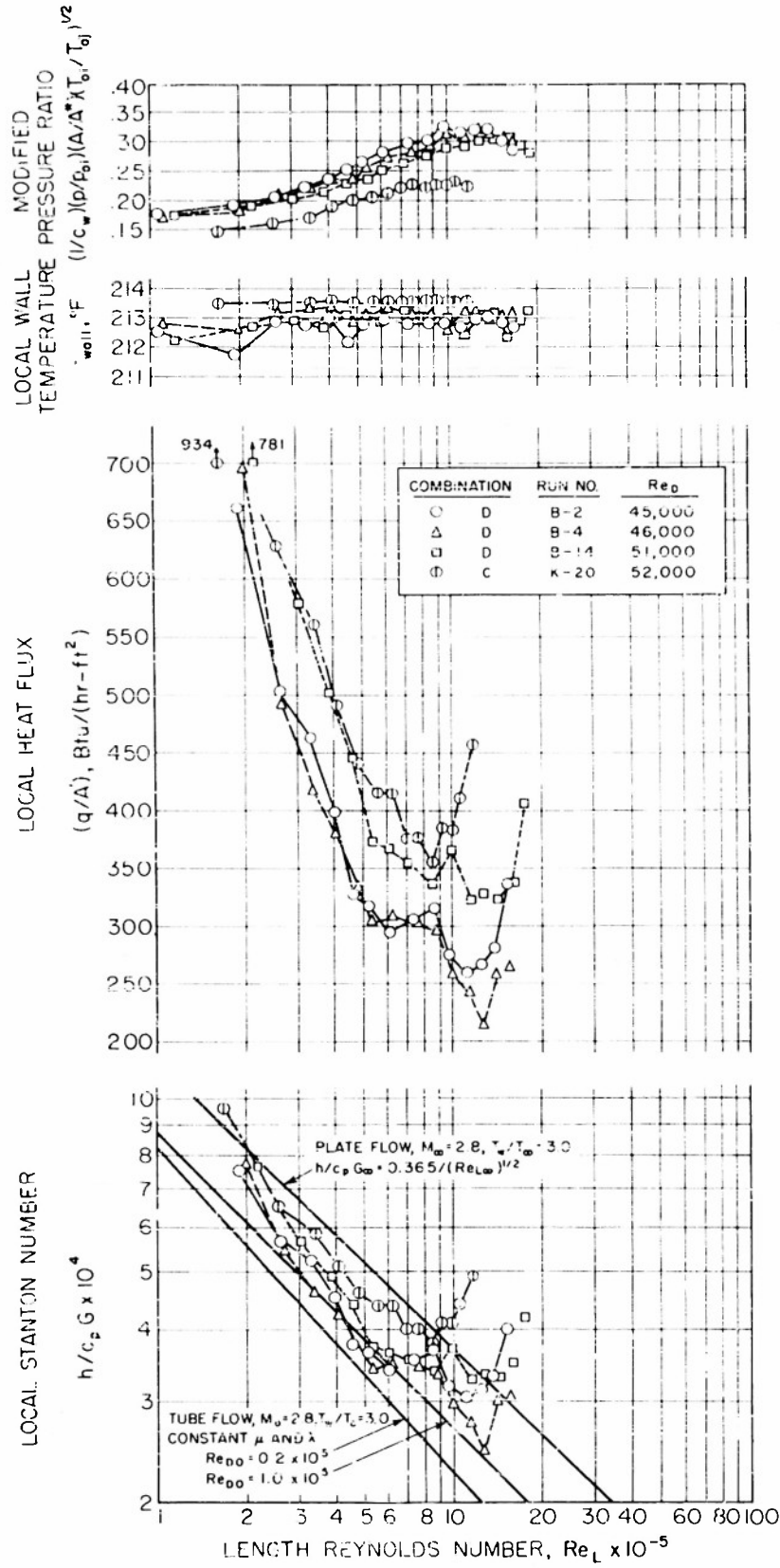


FIGURE 11

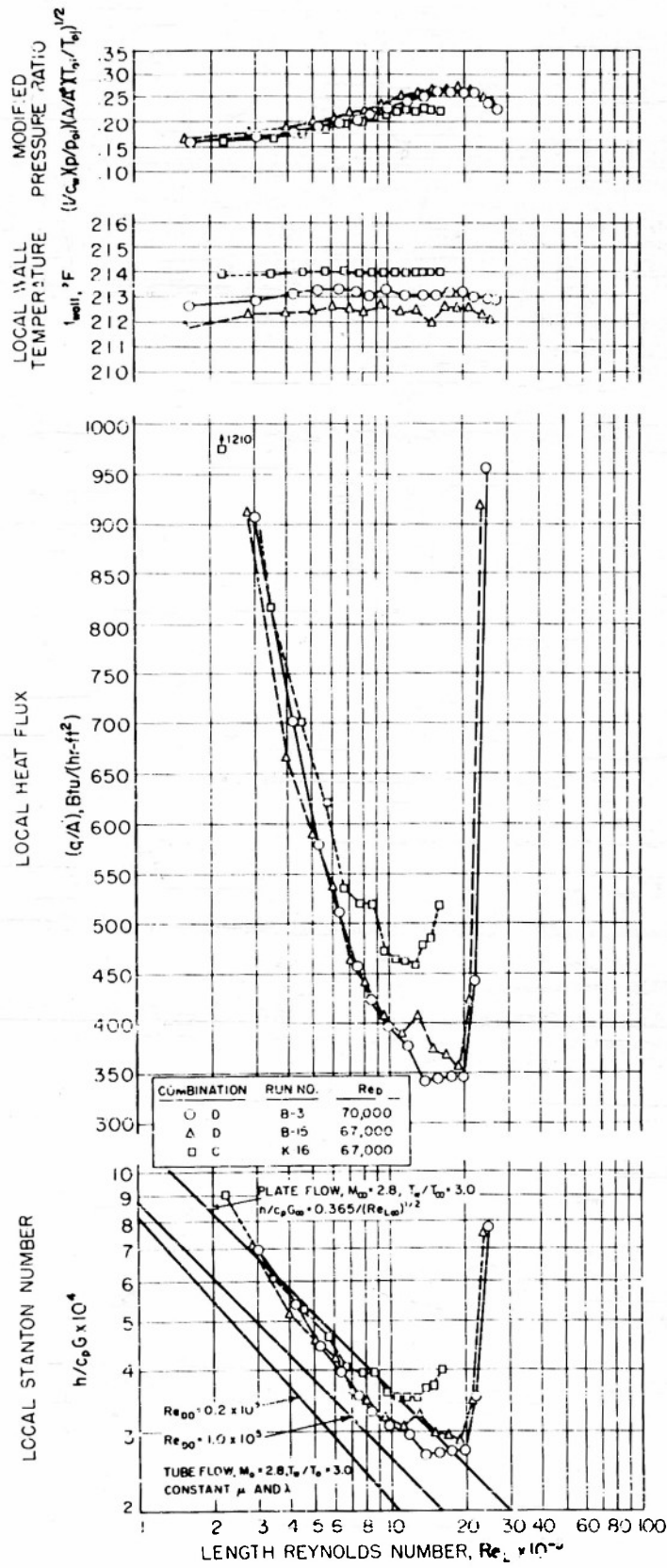


FIGURE 12



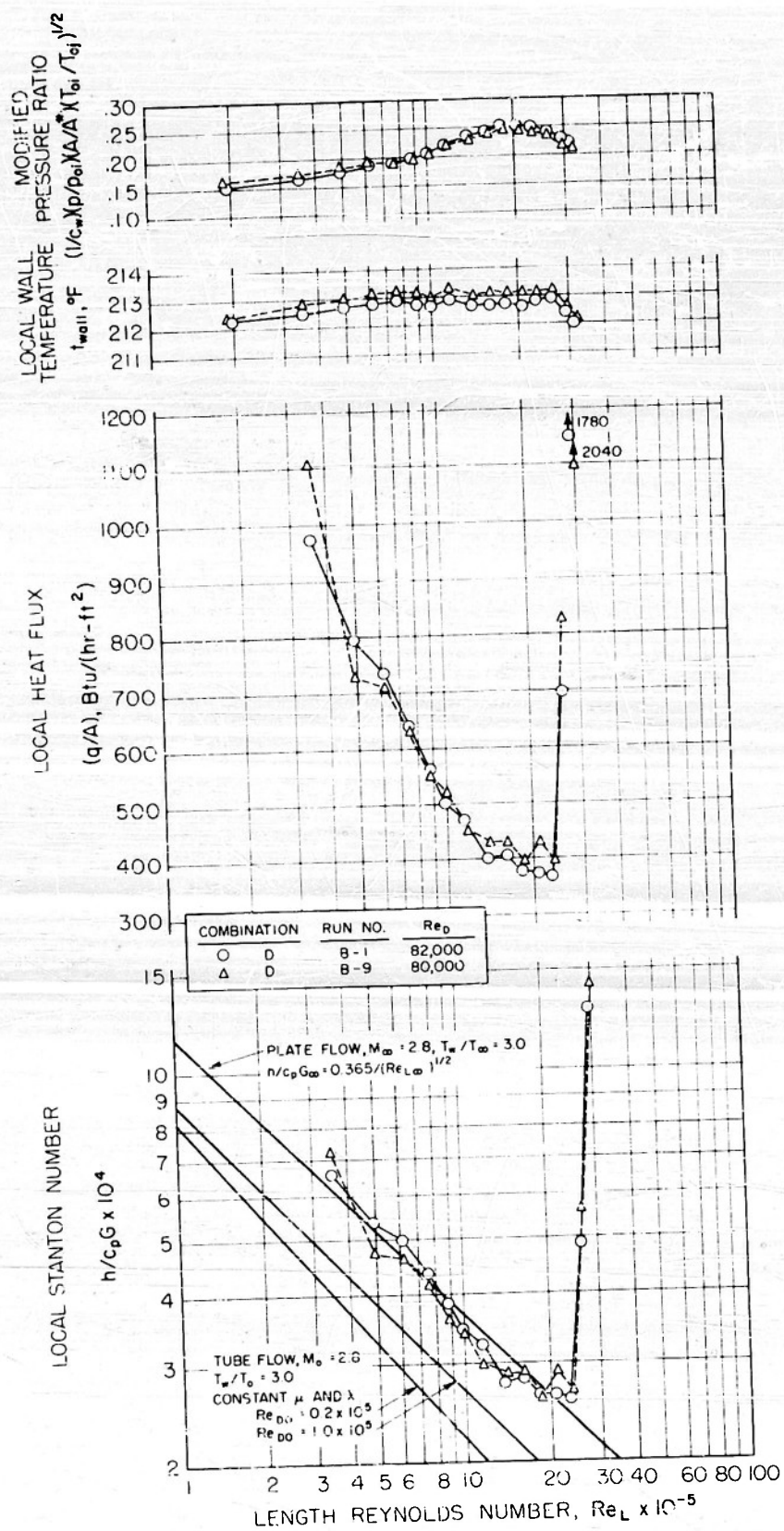


FIGURE 13



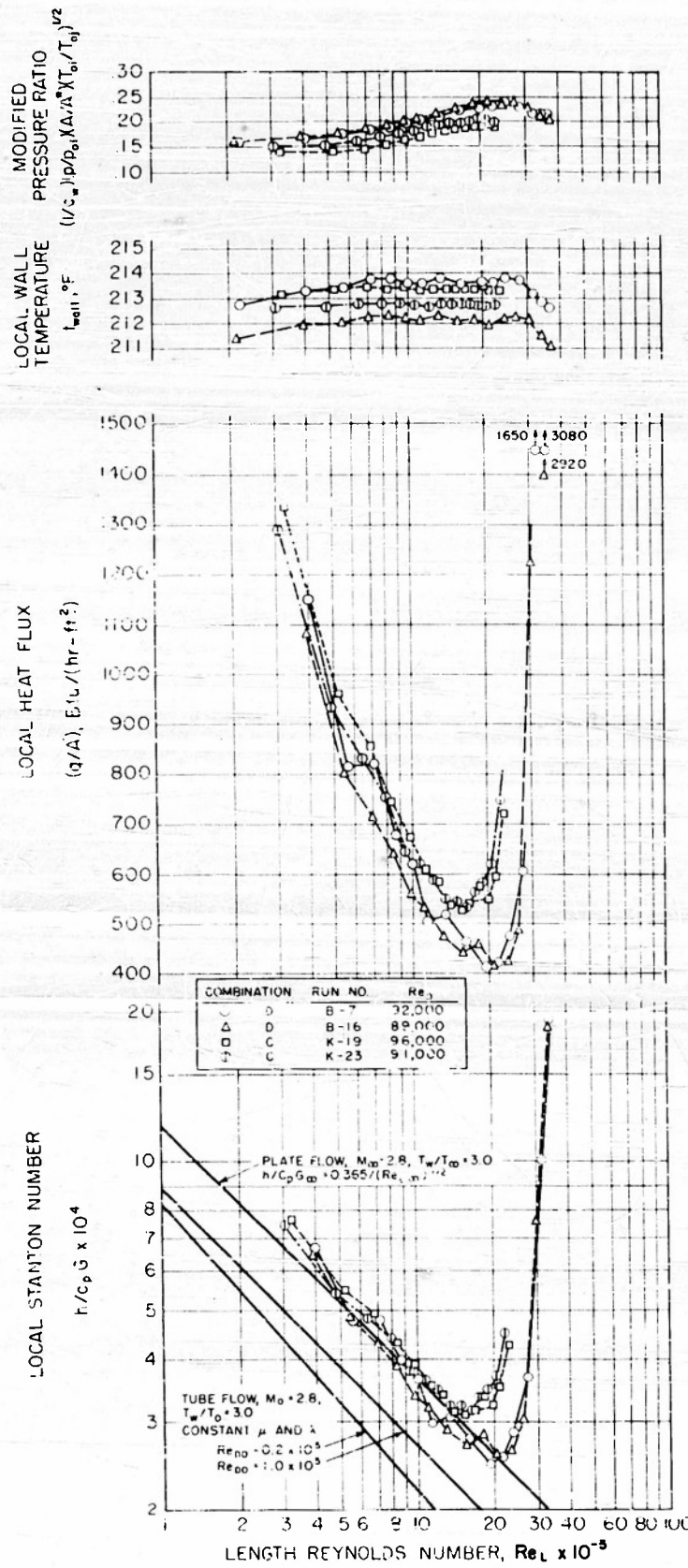


FIGURE 14

# Armed Services Technical Information Agency

Because of our limited supply, you are requested to return this copy WHEN IT HAS SERVED YOUR PURPOSE so that it may be made available to other requesters. Your cooperation will be appreciated.

AD

45686

NOTICE: WHEN GOVERNMENT OR OTHER DRAWINGS, SPECIFICATIONS OR OTHER DATA ARE USED FOR ANY PURPOSE OTHER THAN IN CONNECTION WITH A DEFINITELY RELATED GOVERNMENT PROCUREMENT OPERATION, THE U. S. GOVERNMENT THEREBY INCURS NO RESPONSIBILITY, NOR ANY OBLIGATION WHATSOEVER; AND THE FACT THAT THE GOVERNMENT MAY HAVE FORMULATED, FURNISHED, OR IN ANY WAY SUPPLIED THE SAID DRAWINGS, SPECIFICATIONS, OR OTHER DATA IS NOT TO BE REGARDED BY IMPLICATION OR OTHERWISE AS IN ANY MANNER LICENSING THE HOLDER OR ANY OTHER PERSON OR CORPORATION, OR CONVEYING ANY RIGHTS OR PERMISSION TO MANUFACTURE, USE OR SELL ANY PATENTED INVENTION THAT MAY IN ANY WAY BE RELATED THERETO.

Reproduced by  
DOCUMENT SERVICE CENTER  
KNOTT BUILDING, DAYTON, 2, OHIO

UNCLASSIFIED